Calculation of Tropic Cyclone Inner Structure Using Quantum Theory with Ultimate Acceleration

Huaiyang Cui

Department of Physics, Beihang University, Beijing, 102206, China

Email: hycui@buaa.edu.cn

(September 26, 2022, submitted to viXra)

Abstract: In analogy with the ultimate speed c, there is an ultimate acceleration β, nobody's acceleration can exceed this limit β, in the solar system, β=2.961520e+10(m/s2). Because this ultimate acceleration is large, any effect related to β will become easy to test, including quantum gravity tests. In this paper, an approach is put forward to connect the ultimate acceleration with quantum theory, as an application, this relativistic model gives out the sunspot cycle to be 10.38 years due to the ultimate acceleration. The same approach is applied to tropic cyclone problems, the simulation was carried out, clearly showing the inner structure of a cyclone, which is very consistent with the famous DIANA cyclone on 12 September 1984 in situ observation measured by an aircraft.

1. Introduction

In general, some quantum gravity proposals [1,2] are extremely hard to test in practice, as quantum gravitational effects are appreciable only at the Planck scale [3]. But ultimate acceleration gives another scheme to deal with quantum gravity effects.

In 1843, German pharmacist H.S. Schwabe found that the growth and decline of sunspots had a period of about 10 years through his observation records of sunspots for more than 20 years. In 1848, J.R. Wolf calculated the monthly sunspot relative number to 1749, thus affirming that the average cycle length of sunspot activity was 11.1 years. In 2019, there are 288 days without sunspots, and 40 consecutive days ahead. On December 25, 2019, two new sunspots appeared in the southern hemisphere of the sun, indicating the arrival of the 25th sunspot cycle, which is expected to reach its peak in July 2025. Although it is known that the cycle of sunspot activity is about 11 years, what drives this non-stop pattern is still a mystery.

In analogy with the ultimate speed c, there is an ultimate acceleration β, nobody's acceleration can exceed this limit β, in the solar system, β=2.961520e+10(m/s^2). Because this ultimate acceleration is large, any effect related to β will become easy to test, including quantum gravity tests. In this paper, an approach is put forward to connect the ultimate acceleration with quantum theory, and is applied to the sunspot cycle and tropic cyclone problems.

2. How to connect the ultimate acceleration with quantum theory

In the relativity, the speed of light c is the ultimate speed, nobody's speed can exceed this limit c. The relativistic velocity u of a particle in the coordinate system ($x_1, x_2, x_3, x_4 = ict$) satisfies

$$u_1^2 + u_2^2 + u_3^2 + u_4^2 = -c^2 \ . \tag{1}$$

No matter what particles (electrons, molecules, neutrons, quarks), their 4-vector velocities all have the same magnitude: $|u|=ic$. All particles gain **equality** because of the same magnitude of the 4-velocity u. The acceleration a of a particle is given by

$$a_1^2 + a_2^2 + a_3^2 = a^2; \quad (a_4 = 0; \quad \because x_4 = ict) \tag{2}$$

Assume that particles have an ultimate acceleration β as the limit, no particle can exceed this acceleration limit β. Subtracting both sides of the above equation by β^2, we have

$$a_1^2 + a_2^2 + a_3^2 - \beta^2 = a^2 - \beta^2; \qquad a_4 = 0 \tag{3}$$

It can be rewritten as

$$[a_1^2 + a_2^2 + a_3^2 + 0 + (i\beta)^2] \frac{1}{1 - a^2/\beta^2} = -\beta^2 \tag{4}$$

Now, the particle has an acceleration whose five components are specified by

$$\alpha_1 = \frac{a_1}{\sqrt{1 - a^2/\beta^2}}; \quad \alpha_2 = \frac{a_2}{\sqrt{1 - a^2/\beta^2}};$$

$$\alpha_3 = \frac{a_3}{\sqrt{1 - a^2/\beta^2}}; \quad \alpha_4 = 0; \quad \alpha_5 = \frac{i\beta}{\sqrt{1 - a^2/\beta^2}}; \tag{5}$$

where α_5 is the newly defined acceleration in five-dimensional space-time ($x_1,x_2,x_3,x_4=ict,x_5$). Thus, we have

$$\alpha_1^2 + \alpha_2^2 + \alpha_3^2 + \alpha_4^2 + \alpha_5^2 = -\beta^2; \quad \alpha_4 = 0 \tag{6}$$

It means that the magnitude of the newly defined acceleration α for every particle takes the same value: $|\alpha|=i\beta$ (constant imaginary number), all particle accelerations gain **equality** for the sake of the same magnitude.

How do resolve the velocity u and acceleration α into x, y, and z components? In a realistic world, a hand can rotate a ball moving around a circular path at constant speed v with constant centripetal acceleration a, as shown in Fig.1(a).

(a)   (b)   right hand chirality
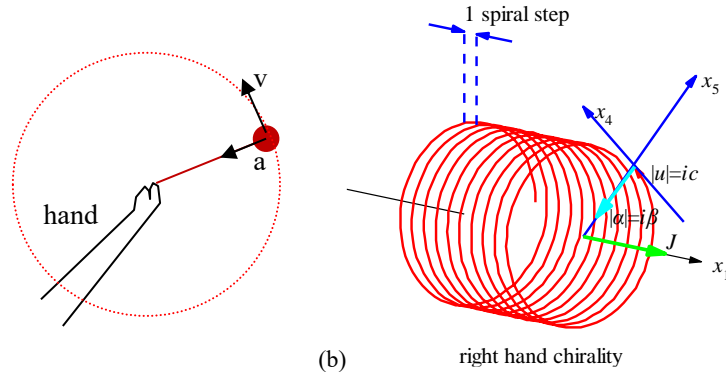
Fig.1   (a) A hand rotates a ball moving around a circular path at constant speed v with constant centripetal acceleration a. (b) The particle moves along the x_1 axis with the constant speed $|u|=ic$ in u direction and constant centripetal force in the x_5 axis at the radius iR (imaginary number).

<Clet2020 Script>//[26]
double D[100],S[2000];int i,j,R,X,N;
int main(){R=50;X=50;N=600;D[0]=-50;D[1]=0;D[2]=0;D[3]=X;D[4]=0;D[5]=0;D[6]=-50;D[7]=R;D[8]=0;

D[9]=600;D[10]=10;D[11]=R;D[12]=0;D[13]=3645;
Lattice(SPIRAL,D,S);SetViewAngle(0,80,-50);DrawFrame(FRAME_NULL,1,0xffffff);
Draw("LINE,0,2,XYZ,0","-150,0,0,-50,0,0");Draw("ARROW,0,2,XYZ,10","50,0,0,150,0,0");
SetPen(2,0xff0000);Plot("POLYLINE,0,600,XYZ",S[9]);i=9+3*N-6;Draw("ARROW,0,2,XYZ,10",S[i]);
TextHang(S[i],S[i+1],S[i+2]," #if|u|=ic#t");TextHang(150,0,0," #ifx#sd1#t");SetPen(2,0x005fff);
Draw("LINE,1,2,XYZ,8","-50,0,50,-50,0,100");Draw("LINE,1,2,XYZ,8","-40,0,50,-40,0,100");
Draw("ARROW,0,2,XYZ,10","-80,0,100,-50,0,100");Draw("ARROW,0,2,XYZ,10","-10,0,100,-40,0,100");
TextHang(-50,0,110,"1 spiral step");i=9+3*N;S[i]=50;S[i+1]=10;S[i+2]=10;
Draw("ARROW,0,2,XYZ,10","50,0,0,50,80,80");TextHang(50,80,80," #ifx#sd5#t");
Draw("ARROW,0,2,XYZ,10","50,72,0,50,0,72");TextHang(50,0,72," #ifx#sd4#t");
SetPen(3,0x00ffff);Draw("ARROW,0,2,XYZ,15",S[i-3]);TextHang(S[i],S[i+1],S[i+2]," #if|α|=iβ#t");
SetPen(3,0x00ff00);Draw("ARROW,0,2,XYZ,15","50,0,0,120,0,0");TextHang(110,5,5," #ifJ#t");
TextHang(-60,0,-80," right hand chirality");}#v07=?>A#t

In analogy with the ball in a circular path, consider a particle in one-dimensional motion along the x_1 axis at the speed v, in Fig.1(b) it moves with the constant speed $|u|=ic$ almost along the x_4 axis and slightly along the x_1 axis, and the constant centripetal acceleration $|\alpha|=i\beta$ in the x_5 axis at the constant radius iR (imaginary number); the coordinate system $(x_1,x_4=ict,x_5=iR)$ establishes a cylinder coordinate system in which this particle moves spirally at the speed v along the x_1 axis. According to the usual centripetal acceleration formula $a=v^2/r$, the acceleration in the x_4-x_5 plane is given by

$$a = \frac{v^2}{r} \quad \Rightarrow \quad i\beta = \frac{|u|^2}{iR} = -\frac{c^2}{iR} = i\frac{c^2}{R} \quad . \tag{7}$$

Therefore, the track of the particle in the cylinder coordinate system $(x_1,x_4=ict,x_5=iR)$ forms a shape, called **acceleration-roll**. The faster the particle moves along the x_1 axis, the longer the spiral step is.

Like a steel spring that contains an elastic wave, the track in the acceleration-roll in Fig.1(b) can be described by a wave function whose phase changes 2π for one spiral step. Apparently, this wave is the de Broglie's matter wave for electrons, protons or quarks, etc.

Theorem: the acceleration-roll bears matter wave.

Proof: The wave function phase changes 2π for one spiral circumference $2\pi(iR)$, then a small displacement of the particle on the spiral track is $|u|d\tau=icd\tau$ in the 4-vector u direction, thus this wave phase along the spiral track is evaluated by

$$phase = \int_0^\tau \frac{2\pi}{2\pi(iR)} icd\tau = \int_0^\tau \frac{c}{R} d\tau \quad . \tag{8}$$

Substituting the radius R into it, the wave function ψ is given by

$$\psi = \exp(-i \cdot phase) = \exp(-i\int_0^\tau \frac{c}{R} d\tau) = \exp(-i\frac{\beta}{c}\int_0^\tau d\tau) \quad . \tag{9}$$

In the theory of relativity, we know that the integral along $d\tau$ needs to transform into a realistic line integral, that is

$$d\tau = -c^2 \frac{d\tau}{-c^2} = (u_1^2 + u_2^2 + u_3^2 + u_4^2)\frac{d\tau}{-c^2}$$
$$= (u_1 dx_1 + u_2 dx_2 + u_3 dx_3 + u_4 dx_4)\frac{1}{-c^2} \quad . \tag{10}$$

Therefore, the wave function ψ is evaluated by

$$\psi = \exp(-i\frac{\beta}{c}\int_0^\tau d\tau)$$

$$= \exp(i\frac{\beta}{c^3}\int_0^x (u_1 dx_1 + u_2 dx_2 + u_3 dx_3 + u_4 dx_4)) \qquad (11)$$

Depending on the particle under investigation, this wave function may have different explanations. If the β is replaced by the Planck constant, the wave function of electrons is given by

$$assume: \quad \beta = \frac{mc^3}{\hbar}$$

$$\psi = \exp(\frac{i}{\hbar}\int_0^x (mu_1 dx_1 + mu_2 dx_2 + mu_3 dx_3 + mu_4 dx_4)) \qquad (12)$$

where $mu_4 dx_4 = -Edt$, it strongly suggests that the wave function is just the de Broglie's matter wave [4,5,6]. The proof is done.

In Fig.1(b), the acceleration-roll of the particle moves with two distinctions: right-hand chirality and left-hand chirality. The direction of the angular momentum J would be slightly different from the x_1 due to spiral precession. It is easy to calculate the ultimate acceleration β, the radius R and the angular momentum J in the plane x_4-x_5 for a spiraling electron as

$$\beta = \frac{c^3 m}{\hbar} = 2.327421\mathrm{e}{+29} \ (\mathrm{M/s}^2); \quad R = \frac{c^2}{\beta} = 3.861593\mathrm{e}{-13} \ (\mathrm{M}) \qquad (13)$$

$$J = \pm m |u| iR = \mp \hbar$$

```
<Clet2020 Script>//[26]
double beta,R,J,m,D[10];char str[200];
int main(){m=ME;beta=SPEEDC*SPEEDC*SPEEDC*m/PLANCKBAR;
R=SPEEDC*SPEEDC/beta;J=PLANCKBAR;Format(str,"beta=%e, #nR=%e, #nJ=%e",beta,R,J);
TextAt(50,50,str);ClipJob(APPEND,str);}#v07=#t
```

Considering another explanation to ψ for planets in the solar system, no Planck constant can be involved. But, in a many-body system with the total mass M, the data analysis [28] tells us that the ultimate acceleration can be rewritten in terms of **Planck-constant-like constant** h as

$$assume: \quad \beta = \frac{c^3}{hM}$$

$$\psi = \exp(\frac{i}{hM}\int_0^x (u_1 dx_1 + u_2 dx_2 + u_3 dx_3 + u_4 dx_4)) \qquad (14)$$

The constant h will be determined by experimental observations. This paper will show that this wave function is applicable to several many-body systems in the solar system, the wave function is called the **acceleration-roll wave**.

Tip: actually, ones cannot get to see the acceleration-roll of a particle in the relativistic space-time $(x_1,x_2,x_3,x_4=ict)$; only get to see it in the cylinder coordinate system $(x_1,x_4=ict,x_5=iR)$.

3. How to determine the ultimate acceleration

In Bohr's orbit model for planets or satellites, as shown in Fig.2, the circular quantization condition

is given in terms of relativistic matter wave in gravity by

$$\left.\begin{array}{c} \dfrac{\beta}{c^3}\oint_L v_l\,dl = 2\pi n \\[2mm] v_l = \sqrt{\dfrac{GM}{r}} \end{array}\right\} \quad\Rightarrow\quad \sqrt{r} = \dfrac{c^3}{\beta\sqrt{GM}}\,n; \quad n = 0,1,2,\dots \ . \tag{15}$$
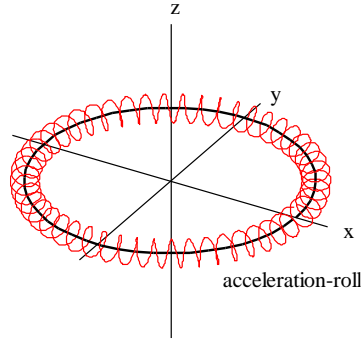

Fig.2   A planet 2D orbit around the sun, an acceleration-roll winding around the planet.

```
<Clet2020 Script>//[26]
int i,j,k; double r,rot,x,y,z,D[20],F[20],S[200]; int main(){SetViewAngle("temp0,theta60,phi-30");
DrawFrame(FRAME_LINE,1,0xafffaf);r=80;Spiral(); TextHang(r,-r,0,"acceleration-roll");
r=110;TextHang(r,0,0,"x");TextHang(0,r,0,"y");TextHang(0,0,r,"z");}
Spiral(){r=80;j=10;rot=j/r;k=2*PI/rot+1;
for(i=0;i<k;i+=1) {D[0]=x;D[1]=y;D[2]=z;D[6]=x;D[7]=y;D[8]=r;
x=r*cos(rot*i);y=r*sin(rot*i);z=0;if(i==0) continue;
SetPen(2,0x00);F[0]=D[0];F[1]=D[1];F[2]=x;F[3]=y;Draw("LINE,0,2,XY,",F);SetPen(1,0xff0000);
D[3]=x;D[4]=y;D[5]=z; D[9]=40;D[10]=10;D[11]=8;D[12]=0;D[13]=360;
Lattice(SPIRAL,D,S);Plot("POLYLINE,0,40,XYZ",S[9]);}
}#v07=?>A#t
```

The solar system, Jupiter's satellites, Saturn's satellites, Uranus' satellites, and Neptune's satellites as five different many-body systems are investigated with Bohr's orbit model. After fitting observational data as shown in Fig.3, their ultimate accelerations are obtained in Table 1. The predicted quantization blue-lines in Fig.3(a), Fig.3(b), Fig.3(c), Fig.3(d) and Fig.3(e) agree well with experimental observations for those *inner constituent planets or satellites*.
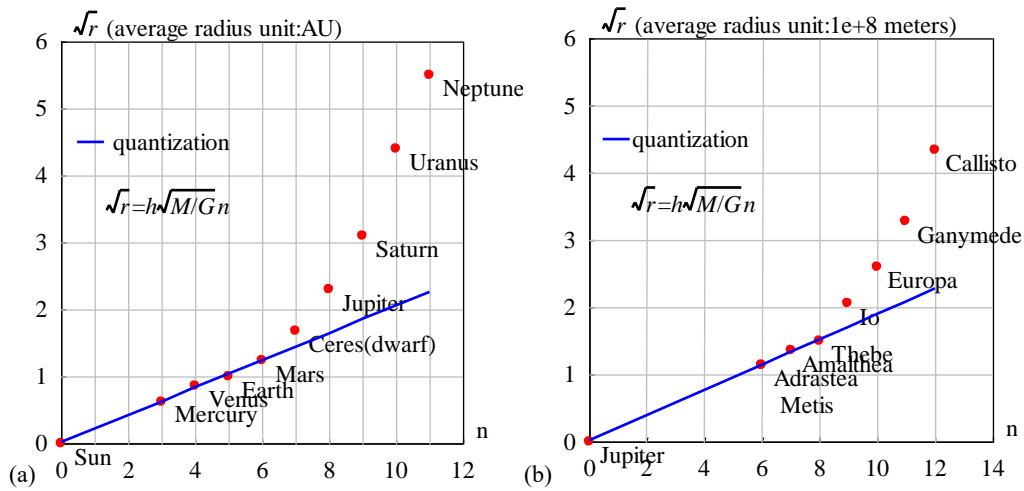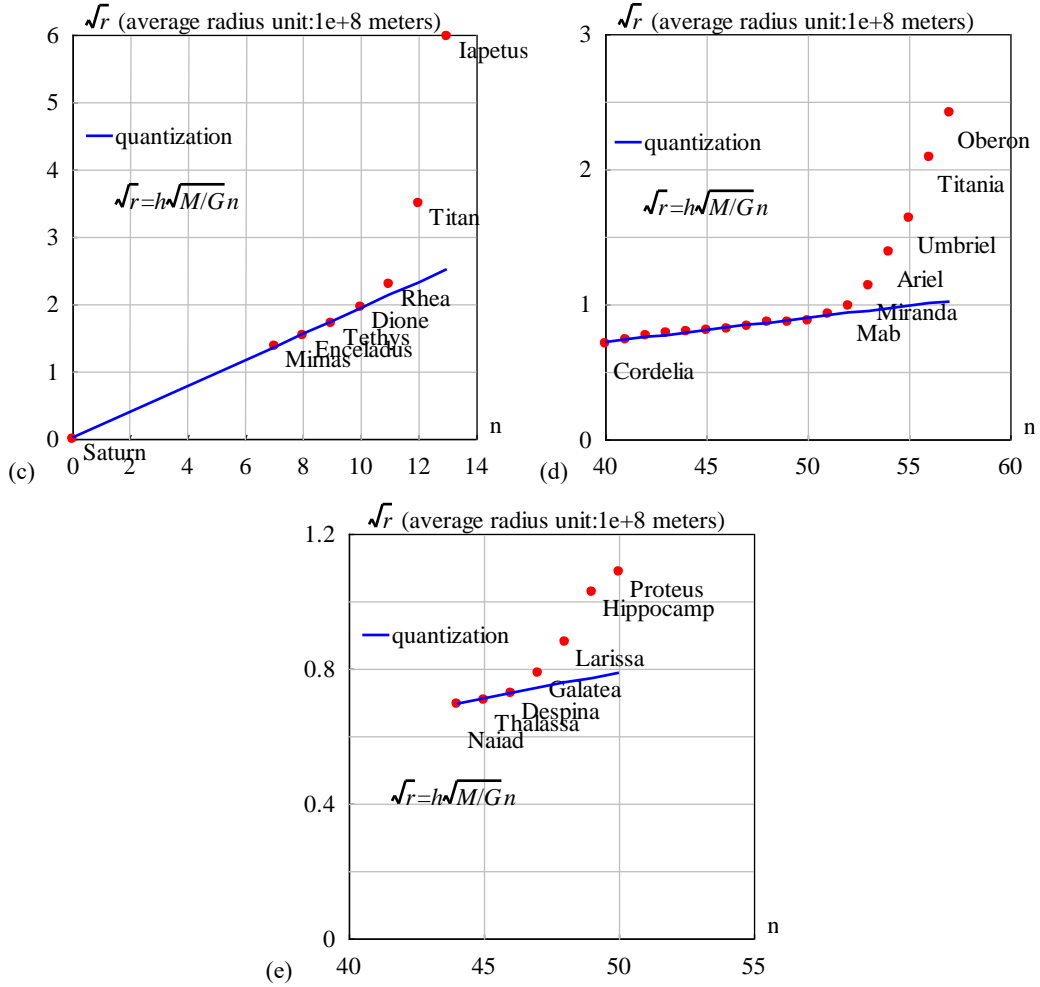
Fig.3 The orbital radii are quantized for inner constituents. (a) the solar system with h=4.574635e-16 ($m^2 s^{-1} kg^{-1}$). The relative error is less than 3.9%. (b) the Jupiter system with h=3.531903e-16 ($m^2 s^{-1} kg^{-1}$). Metis and Adrastea are assigned the same quantum number for their almost same radius. The relative error is less than 1.9%. (c) the Saturn system with h=6.610920e-16 ($m^2 s^{-1} kg^{-1}$). The relative error is less than 1.1%. (d) the Uranus system with h=1.567124e-16 ($m^2 s^{-1} kg^{-1}$). n=0 is assigned to Uranus. The relative error is less than 2.5%. (e) the Neptune system with h=1.277170e-16 ($m^2 s^{-1} kg^{-1}$). n=0 is assigned to Neptune. The relative error is less than 0.17%.

Table 1 Planck-constant-like constant h, N is constituent particle number with smaller orbital inclination.

system	N	M/M_{earth}	β (m/s2)	h (m2s-1kg-1)	Prediction
Solar planets	9	333000	2.961520e+10	4.574635e-16	Fig.3(a)
Jupiter' satellites	7	318	4.016793e+13	3.531903e-16	Fig.3(b)
Saturn's satellites	7	95	7.183397e+13	6.610920e-16	Fig.3(c)
Uranus' satellites	18	14.5	1.985382e+15	1.567124e-16	Fig.3(d)
Neptune 's satellites	7	17	2.077868e+15	1.277170e-16	Fig.3(e)

Besides every β, our interest shifts to the constant h in Table 1, which is defined as

$$h = \frac{c^3}{M\beta} \quad \Rightarrow \quad \sqrt{r} = h\sqrt{\frac{M}{G}}n \ . \tag{16}$$

In a many-body system with a total mass of M, a constituent particle has the mass of m and moves

at the speed of v, it is easy to find that the wavelength of de Broglie's matter wave should be modified for planets and satellites as

$$\lambda_{de\_Broglie} = \frac{2\pi\hbar}{mv} \Rightarrow \text{modify} \Rightarrow \lambda = \frac{2\pi hM}{v} \quad . \tag{17}$$

where h is a **Planck-constant-like constant**. Usually, the total mass M is approximately equal to the central-star's mass. It is found that this modified matter wave works for quantizing orbits correctly in Fig.3 [28,29]. The key point is that the various systems have almost the same Planck-constant-like constant h in Table 1 with a mean value of 3.51e-16 $m^2s^{-1}kg^{-1}$, at least having the same magnitude! The acceleration-roll wave is a generalized matter wave as a planetary scale wave.

In Fig.3(a), the blue straight line expresses the linear regression relation among the Sun, Mercury, Venus, Earth and Mars, their quantization parameters are hM=9.098031e+14(m^2/s). The ultimate acceleration is fitted out to be β=2.961520e+10 (m/s^2). Where, n=3,4,5,.. were assigned to solar planets, the sun was assigned a quantum number n=0 because the sun is in the **central state**.

4. Optical model of the central state

The acceleration-roll wave as the relativistic matter wave generalized in gravity is given by

$$\psi = \exp(\frac{i}{hM}\int_0^x v_l dl); \quad \lambda = \frac{2\pi hM}{v_l} = \frac{2\pi c^3}{v_l\beta} \quad . \tag{18}$$

In a central state n=0, if the coherent length of the acceleration-roll wave is long enough, its head may overlap with its tail when the particle moves in a closed orbit in space-time, as shown in Fig.4, the interference of the acceleration-roll wave between its head and tail will occur in the overlapping zone. The overlapped wave is given by

$$\psi(r) = 1 + e^{i\delta} + e^{i2\delta} + ... + e^{i(N-1)\delta} = \frac{1 - \exp(iN\delta)}{1 - \exp(i\delta)}$$

$$\delta(r) = \frac{1}{hM}\oint_L (v_l)dl = \frac{2\pi\omega r^2}{hM} = \frac{2\pi\beta\omega r^2}{c^3} \tag{19}$$

where N is the overlapping number which is determined by the coherent length of the acceleration-roll wave, δ is the phase difference after one orbital motion, ω is the angular speed of the solar rotation. The above equation is a multi-slit interference formula in optics, for a larger N it is called the Fabry-Perot interference formula.
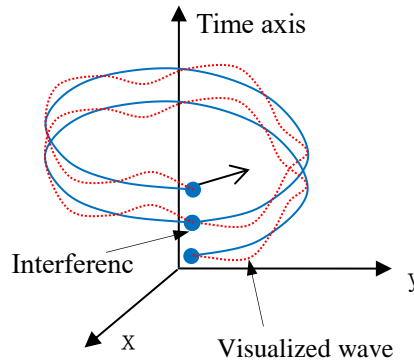

Fig.4   The head of the acceleration-roll wave may overlap with its tail.

The acceleration-roll wave function ψ needs a further explanation. In quantum mechanics, $|\psi|^2$ equals to the probability of finding an electron due to Max Burn's explanation; in astrophysics, $|\psi|^2$ equals to the probability of finding a nucleon (proton or neutron) *averagely on an astronomic scale*, because all mass is mainly made of nucleons, we have

$$|\psi|^2 \propto nucleon\_density \,. \tag{20}$$

It follows from the multi-slit interference formula that the interference intensity at maxima is proportional to N^2, that is

$$N^2 = \frac{|\psi(0)_{multi-wavelet}|^2}{|\psi(0)_{one-wavelet}|^2} \,. \tag{21}$$

What matter plays the role of "one-wavelet" in the solar core or earth core? We choose air-vapor at the sea level on the earth's surface as the "reference matter: one-wavelet". Thus, the overlapping number N is estimated by

$$N^2 = \frac{|\psi(0)_{multi-wavelet}|^2}{|\psi(0)_{one-wavelet}|^2} \approx \frac{core\_nucleon\_density_{r=0}}{air\_vapor\_density_{r=sea}} \,. \tag{22}$$

Although today there is no air-vapor on the solar surface, the solar core has a maximum density of 1.5e+5kg/m^3 [31], comparing to the air-vapor density of 1.29 kg/m^3 at the sea level on the earth, the solar overlapping number N is estimated as N=341. The earth's core density is 5.53e+3kg/m^3, the earth's overlapping number N is estimated as N=65.

For the Sun, Earth and Mars, their central densities and their reference matter density are given in Table 2. Thus, their overlapping numbers are estimated also in this table.

Sun's rotation angular speed at the equator is known as ω=2π/(25.05*24*3600), unit: s^{-1}. Its mass 1.9891e+30 (kg), radius 6.95e+8 (m), mean density 1408 (kg/m^3), the solar core has a maximum density of 1.5e+5kg/m^3 [31], the ultimate acceleration β=2.961520e+10 (m/s^2), the constant hM= 9.100745e+14 (m^2/s). According to the N=341, the matter distribution of the $|\psi|^2$ is calculated in Fig.5, it agrees well with the general description of the sun's interior. The radius of the sun is calculated to be r=7e+8 (m) with a relative error of 0.72% in Fig.5, which indicates that the sun radius strongly depends on the sun's self-rotation.

Table 2   Estimating the overlapping number N by comparing solid core to reference matter, regarding protons and neutrons as basis particles.

| object	Solid core, density (kg/m^3)	Reference matter, density (kg/m^3)	Overlapping number N	β (m/s^2)
Sun	1.5e+5 (max.)	1.29 (vapor above the sea)	341	2.961520e+10
Earth	5530	1.29 (vapor above the sea)	65	1.377075e+14
Mars	3933.5	1.29 (vapor above the sea)	55	2.581555e+15
Jupiter	1326			4.016793e+13
Saturn	687			7.183397e+13
Uranus	1270			1.985382e+15
Neptune	1638			2.077868e+15
Alien-planet	5500	1.29(has water on the surface)	65	
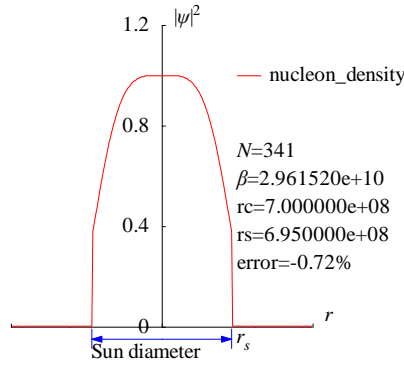
Fig.5 The matter distribution |ψ|2 around the Sun has been calculated in the radius direction.

```
<Clet2020 Script>//[26]
int i,j,k,m,n,N,nP[10];
double beta,H,B,M,r,r_unit,x,y,z,delta,D[1000],S[1000], a,b,rs,rc,rot,atm_height; char str[100];
main(){k=150;rs=6.95e8;rc=0;x=25.05;rot=2*PI/(x*24*3600);n=0; N=341;
beta=2.961520e10;H=SPEEDC*SPEEDC*SPEEDC/beta;M=1.9891E30; atm_height=2e6; r_unit=1E7;
b=PI/(2*PI*rot*rs*rs/H);
for(i=-k;i<k;i+=1) {r=abs(i)*r_unit;
if(r<rs+atm_height) delta=2*PI*rot*r*r/H; else delta=2*PI*sqrt(GRAVITYC*M*r)/H;//around the star
y=SumJob("SLIT_ADD,@N,@delta",D); y=y/(N*N);
S[n]=i;S[n+1]=y; if(i>0 && rc==0 && y<0.001) rc=r;D[n]=i;D[n+1]=z;n+=2;}
SetAxis(X_AXIS,-k,0,k,"#ifr; ; ; ;");SetAxis(Y_AXIS,0,0,1.2,"#if|ψ|#su2#t;0;0.4;0.8;1.2;");
DrawFrame(FRAME_SCALE,1,0xafffaf); z=100*(rs-rc)/rs;
SetPen(1,0xff0000);Polyline(k+k,S,k/2,1," nucleon_density"); SetPen(1,0x0000ff); //Polyline(k+k,D);
//Draw("LINE,0,2,XY,0","20,0.5,60,0.6");TextHang(60,0.6,0,"core");
r=rs/r_unit;y=-0.05;D[0]=-r;D[1]=y;D[2]=r;D[3]=y; Draw("ARROW,3,2,XY,10,100,10,10,",D);
Format(str,"#ifN#t=%d#n#ifβ#t=%e#nrc=%e#nrs=%e#nerror=%.2f%",N,beta,rc,rs,z);
TextHang(k/2,0.7,0,str);TextHang(r+5,y/2,0,"#ifr#sds#t");TextHang(-r,y+y,0,"Sun diameter");
}#v07=?>A#t
```

5.   Earth's central state and space debris distribution

Appling the acceleration-roll wave to the Moon, as illustrated in Fig.6(a), the Moon has been assigned a quantum number of $n=2$ in the author's early study [28]. According to the quantum condition, the ultimate acceleration is fitted out to be $β=1.377075e+14$ (m/s^2) in the earth system. Another consideration is to take the quasi-satellite's perigee into account, for the moon and 2004_GU9 etc., as shown in Fig.6(b), but this consideration requires further understanding of its five quasi-satellites [28].
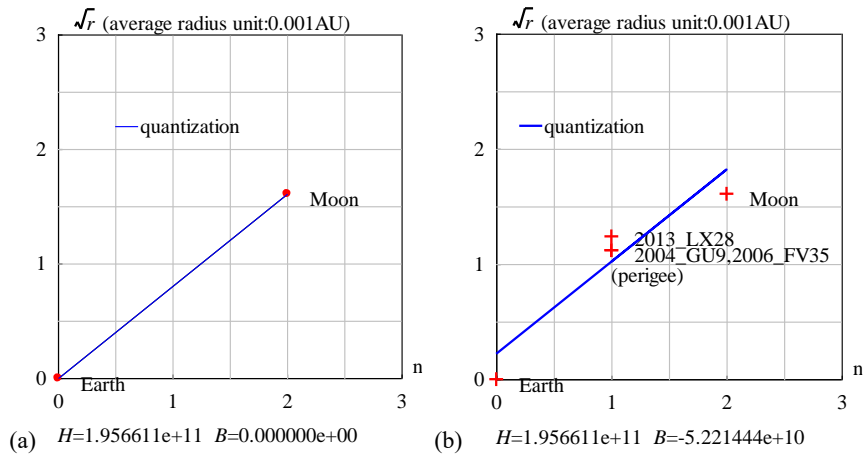

Fig.6   orbital quantization for moon and quasi-satellites to the Earth, $H=hM$.

```
<Clet2020 Script>//[26]
char str[200];int i,j,k,N,nP[10]; double x,y,z,M,r_unit,a,b,B,H,r_ave[20],dP[10],D[1000];
double orbit[10]={0,2.57,0,}; double e[10]={0, 0.0549,0,0,0,0,0,0,0,0,};
int qn[10]={0,2,3,4,5,6,7,8,9.,10,}; char Stars[100]={"Earth;Moon;"};
int main(){ N=2; M=5.97237E24; r_unit=1.495978707e8;
```

9

```
for(i=0;i<N;i+=1) {x=orbit[i];y=e[i]; z=x*(1+sqrt(1-y*y))/2;r_ave[i]=z;//average_radius
D[i+i]=qn[i];D[i+i+1]=sqrt(z); }
DataJob("REGRESSION,2",D,dP);b=dP[0];a=dP[1];
SetAxis(X_AXIS,0,0,3,"n;0;1;2;3;");
SetAxis(Y_AXIS,0,0,3," #if#rsr#t (average radius unit:0.001AU);0;1;2;3;");
DrawFrame(0x0166,1,0xafffaf); Polyline(N,D);
SetPen(2,0xff0000); Plot("OVALFILL,0,2,XY,3,3,",D);
for(i=0;i<N;i+=1) {nP[0]=TAKE;nP[1]=i;TextJob(nP,Stars,str);x=qn[i]+0.2;y=sqrt(orbit[i])-0.05;TextHang(x,y,0,str);}
x=GRAVITYC*M*r_unit;z=sqrt(x);H=z*a;B=-z*b;
TextAt(100,450,"#ifH#t=%e   #ifB#t=%e",H,B);
for(i=0;i<N;i+=1) {y=b+a*qn[i];D[i+i]=qn[i];D[i+i+1]=y;}
SetPen(1,0x0000ff);Polyline(N,D,0.5,2.2,"quantization");//check
}}#v07=?>A#t
```

The earth's rotation angular speed is known as $\omega=2\pi/(24*3600)$, unit s^{-1}. Its mass 5.97237e+24(kg), radius 6.371e+6(m), core density 5530(kg/m^3), the ultimate acceleration β=1.377075e+14(m/s^2), the constant hM=1.956611e+11(m^2/s).

We have estimated that the wave overlapping number in the central state of the earth is N=65, the matter distribution $|\psi|^2$ in radius direction is calculated as shown in Fig.7(a), where the self-rotation near its equator has the period of 24 hours:

$$\delta(r) = \frac{1}{hM}\oint_L (v_l)dl = \frac{2\pi r}{hM}\omega r = \frac{2\pi\beta\omega r^2}{c^3} \quad . \tag{23}$$

There is a central maximum of matter distribution at the earth's heart, which gradually decreases to zero near the earth's surface, then rises the secondary peaks and attenuates down off. The radius of the earth is calculated to be r=6.4328e+6 (m) with a relative error of 0.86% using the interference of its acceleration-roll wave. Space debris over the atmosphere has a complicated evolution [7,8], and has itself speed

$$v_l = \sqrt{\frac{GM}{r}}; \quad \delta(r) = \frac{1}{hM}\oint_L (v_l)dl = \frac{\beta}{c^3}\oint_L (v_l)dl = \frac{2\pi\beta}{c^3}\sqrt{GMr} \quad . \tag{24}$$

The secondary peaks over the atmosphere up to 2000km altitude are calculated in Fig.7(b) which agrees well with the space debris observations [16]; the peak near 890 km altitude is due principally to the January 2007 intentional destruction of the FengYun-1C weather spacecraft while the peak centered at approximately 770 km altitude was created by the February 2009 accidental collision of Iridium 33 (active) and Cosmos 2251 (derelict) communication spacecraft [16,18]. The observations based on the incoherent scattering radar EISCAT ESR located at 78°N in Jul. 2006 and in Oct. 2015 [21,22,23] are respectively shown in Fig.7(c) and (d). This prediction of secondary peaks also agrees well with other space debris observations [24,25].
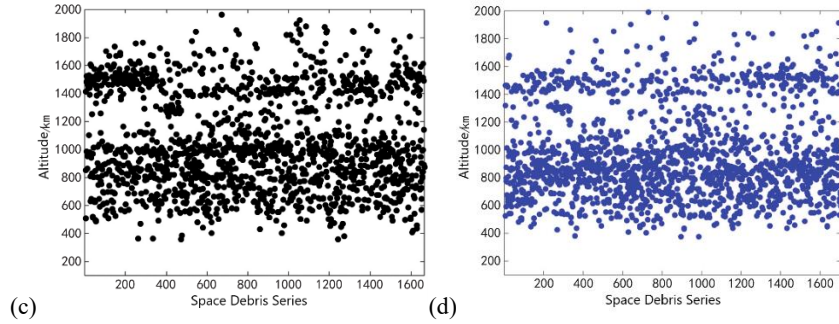

(a)

(b)
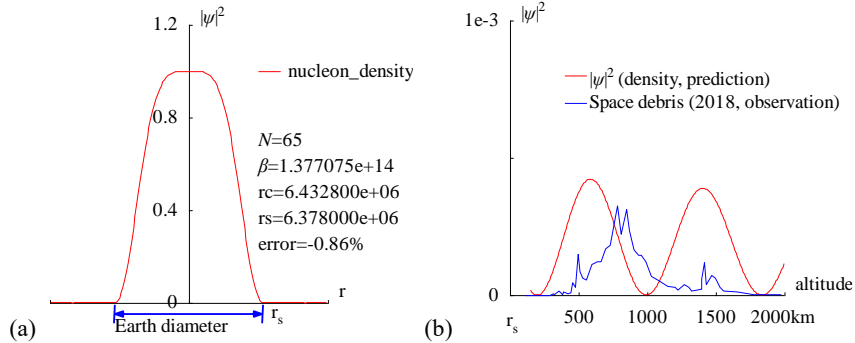
Fig.7 (a) The radius of the Earth is calculated out r=6.4328e+6 (m) with a relative error of 0.86% by the interference of its acceleration-roll wave; (b) The prediction of the space debris distribution up to 2000km altitude; (c) The pace debris distribution in Jul. 2006, Joint observation based on the incoherent scattering radar EISCAT ESR located at 78°N [21]; (d) The space debris distribution in Oct. 2015, Joint observation based on the incoherent scattering radar EISCAT ESR located at 78°N [21].

```
<Clet2020 Script>//[26]
int i,j,k,m,n,N,nP[10]; double H,B,M,v_r,r,AU,r_unit,x,y,z,delta,D[10],S[1000];
double rs,rc,rot,a,b,atm_height,beta; char str[100];
main(){k=80;rs=6.378e6;rc=0;atm_height=1.5e5;n=0; N=65;
beta=1.377075e+14;H=SPEEDC*SPEEDC*SPEEDC/beta;
M=5.97237e24;AU=1.496E11;r_unit=1e-6*AU; rot=2*PI/(24*60*60);//angular speed of the Earth
for(i=-k;i<k;i+=1) {r=abs(i)*r_unit;
if(r<rs+atm_height) v_r=rot*r*r; else v_r=sqrt(GRAVITYC*M*r);//around the Earth
delta=2*PI*v_r/H; y=SumJob("SLIT_ADD,@N,@delta",D); y=y/(N*N);
if(y>1) y=1; S[n]=i;S[n+1]=y; if(i>0 && rc==0 && y<0.001) rc=r;    n+=2;}
SetAxis(X_AXIS,-k,0,k,"r; ; ; ;");SetAxis(Y_AXIS,0,0,1.2,"#if|ψ|#su2#t;0;0.4;0.8;1.2;");
DrawFrame(FRAME_SCALE,1,0xafffaf); x=50;z=100*(rs-rc)/rs;
SetPen(1,0xff0000);Polyline(k+k,S,k/2,1," nucleon_density");
r=rs/r_unit;y=-0.05;D[0]=-r;D[1]=y;D[2]=r;D[3]=y;
SetPen(2,0x0000ff); Draw("ARROW,3,2,XY,10,100,10,10,",D);
Format(str,"#ifN#t=%d#n#ifβ#t=%e#nrc=%e#nrs=%e#nerror=%.2f%",N,beta,rc,rs,z);
TextHang(k/2,0.7,0,str);TextHang(r+5,y/2,0,"r#sds#t");TextHang(-r,y+y,0,"Earth diameter");
}#v07=?>A#t


<Clet2020 Script>//[26]
int i,j,k,m,n,N,nP[10]; double H,B,M,v_r,r,AU,r_unit,x,y,z,delta,D[10],S[10000];
double rs,rc,rot,a,b,atm_height,p,T,R1,R2,R3; char str[100]; int
Debris[96]={110,0,237,0,287,0,317,2,320,1,357,5,380,1,387,4,420,2,440,3,454,14,474,9,497,45,507,26,527,19,557,17,597,34,63
4,37,664,37,697,51,727,55,781,98,808,67,851,94,871,71,901,50,938,44,958,44,991,37,1028,21,1078,17,1148,10,1202,9,1225,6,
1268,12,1302,9,1325,5,1395,7,1395,18,1415,36,1429,12,1469,22,1499,19,1529,9,1559,5,1656,4,1779,1,1976,1,};
main(){k=80;rs=6.378e6;rc=0;atm_height=1.5e5;n=0; N=65;
H=1.956611e11;M=5.97237e24;AU=1.496E11;r_unit=1e4;
rot=2*PI/(24*60*60);//angular speed of the Earth
b=PI/(2*PI*rot*rs*rs/H); R1=rs/r_unit;R2=(rs+atm_height)/r_unit;R3=(rs+2e6)/r_unit;
for(i=R2;i<R3;i+=1) {r=abs(i)*r_unit; delta=2*PI*sqrt(GRAVITYC*M*r)/H;
y=SumJob("SLIT_ADD,@N,@delta",D); y=1e3*y/(N*N);// visualization scale:1000
if(y>1) y=1; S[n]=i;S[n+1]=y;n+=2;}
SetAxis(X_AXIS,R1,R1,R3,"altitude: r#sds#t;500;1000;1500;2000km ;");
SetAxis(Y_AXIS,0,0,1,"#if|ψ|#su2#t;0; ;1e-3;");DrawFrame(FRAME_SCALE,1,0xafffaf); x=R1+(R3-R1)/5;
SetPen(1,0xff0000);Polyline(n/2,S,x,0.8,"#if|ψ|#su2#t (density, prediction)");
for(i=0;i<48;i+=1) {S[i+i]=R1+(R3-R1)*Debris[i+i]/2000; S[i+i+1]=Debris[i+i+1]/300;}
SetPen(1,0x0000ff);Polyline(48,S,x,0.7,"Space debris (2018, observation) "); }#v07=?>A#t
```

6. Mars and Jovian planets

Mars and its satellites are quantized very well by its ultimate acceleration β as shown in Fig.8(a). Now let us talk about Mars in the central state with quantum number $n=0$, its ultimate acceleration is β=2.581555e+15(m/s^2) in the Mars system. We have estimated Mars' overlapping number N=55 in Table 2, the matter distribution $|\psi|^2$ around Mars can be calculated in the radial direction as shown in Fig.8(b), where the self-rotation at the equator has a period of 24 hours.

The radius of Mars is calculated as r=1.6e+6 (m) with a relative error of 52.79%, no further attempt was made to improve the calculation, because of limited knowledge about Mars history. But one thing is certain, Mars has frequently been bombarded with smaller objects, in fact, consequently

with the inclination of 25.2 degrees, so that its self-rotation is unstable or incorrect for its formation in a sense.
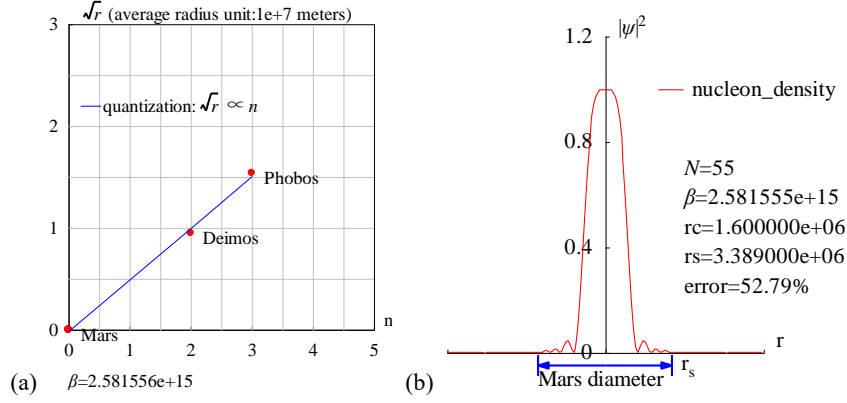

Fig.8 (a)Quantization of Mars and its satellites. (b)The matter distribution $|\psi|^2$ around Mars has been calculated in the radius direction.

```
<Clet2020 Script>//[26]
int i,j,k,m,n,N,nP[10];
double H,B,M,v_r,r,AU,r_unit,x,y,z,delta,D[10],S[1000],F[1000];
double rs,rc,rot,a,b,atm_height,beta; char str[100];
main(){k=80;rs=3.389e6;rc=0;atm_height=10e3;n=0; N=55;
beta=2.581555e15; H=SPEEDC*SPEEDC*SPEEDC/beta;
M=0.107*5.97237e24; AU=1.496E11;r_unit=1e5;
rot=2*PI/(24*60*60);//angular speed
for(i=-k;i<k;i+=1) {r=abs(i)*r_unit;
if(r<rs+atm_height) v_r=rot*r*r; else v_r=sqrt(GRAVITYC*M*r);//around the star
delta=2*PI* v_r/H;y=SumJob("SLIT_ADD,@N,@delta",D); y=y/(N*N);
if(y>1) y=1; S[n]=i;S[n+1]=y; if(i>0 && rc==0 && y<0.001) rc=r;   n+=2;}
SetAxis(X_AXIS,-k,0,k,"r; ; ; ;");SetAxis(Y_AXIS,0,0,1.2,"#if|\psi|#su2#t;0;0.4;0.8;1.2;");
DrawFrame(FRAME_SCALE,1,0xafffaf); x=50;z=100*(rs-rc)/rs;
SetPen(1,0xff0000);Polyline(k+k,S,k/3,1," nucleon_density");
r=rs/r_unit;y=-0.05;D[0]=-r;D[1]=y;D[2]=r;D[3]=y;
SetPen(2,0x0000ff); Draw("ARROW,3,2,XY,10,100,10,10,",D);
Format(str,"#ifN#t=%d#n#ifβ#t=%e#nrc=%e#nrs=%e#nerror=%.2f%",N,beta,rc,rs,z);
TextHang(k/2,0.7,0,str);TextHang(r+5,y/2,0,"r#sds#t"); TextHang(-r,y+y,0,"Mars diameter");
}#v07=?>A#t
```

To extend the quantization rule to the Jovian planets (Jupiter, Saturn, Uranus and Neptune), it is necessary to further study the magnet-like components of gravity [28], an issue beyond the scope of this paper.

7. Sunspot cycle

The **coherence length** of waves is usually mentioned but the **coherence width** of waves is rarely discussed in quantum mechanics, simply because the latter is not a matter for electrons, nucleon, or photos, but it is a matter in astrophysics. The analysis of observation data tells us that on the planetary scale, the coherence width of acceleration roll waves can be extended to 1000 kilometers or more, as illustrated in Fig.9(a), the overlap may even occur in the width direction, thereby bringing new aspects to wave interference.

In the solar convective zone, adjacent convective arrays form a top-layer flow, a middle-layer gas, and a ground-layer flow, similar to the concept of **molecular current** in electromagnetism. Considering one convective ring at the equator as shown in Fig.9(b), there is an apparent velocity difference between the top-layer flow and the middle-layer gas, where their acceleration-roll waves are denoted respectively by
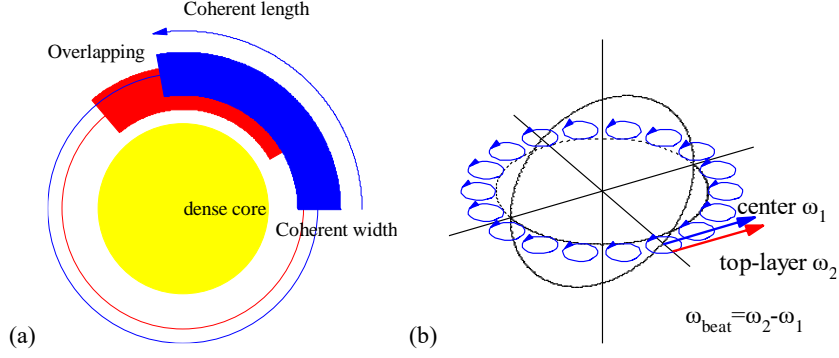
Fig.9   (a) Illustration of overlapping in the coherent width direction. (b) In convective rings at the equator, the speed difference causes a beat frequency.

```
<Clet2020 Script>// [26]
int i, j, k, R,D[500];
main(){DrawFrame(FRAME_NULL,1,0xafffaf);
R=60; SetPen(1,0xffff00);
D[0]=-R; D[1]=-R; D[2]=R; D[3]=R; Draw("ELLIPSE,1,2,XY,0",D);
R=85;   k=15; SetPen(1,0xff0000);
D[0]=-R; D[1]=-R; D[2]=R; D[3]=R; Draw("ELLIPSE,0,2,XY,0",D);
D[0]=0; D[1]=0; D[2]=R-k; D[3]=0; D[4]=R+k;D[5]=0;
Draw("SECTOR,1,3,XY,15,30,130,0",D);
R=95; k=15; SetPen(1,0x00ff);
D[0]=-R; D[1]=-R; D[2]=R; D[3]=R; Draw("ELLIPSE,0,2,XY,0",D);
D[0]=0; D[1]=0; D[2]=R-k; D[3]=0; D[4]=R+k;D[5]=0;
Draw("SECTOR,1,3,XY,15,0,100,0",D);D[4]=R+k+k;
Draw("SECTOR,3,3,XY,15,0,100,0",D);
TextHang(0,0,0,"dense core");TextHang(R-k-k,-k,0,"Coherent width");
TextHang(0,R+k+k,0,"Coherent length");TextHang(-R,R+k,0,"Overlapping");
}#v07=?>A#t


<Clet2020 Script>//Clet is a C compiler[26]
double beta,H,M,N,dP[20],D[2000],r,rs,rot,x,y,v1,v2,K1,K2,T1,T2,T,Lamda,V; int i,j,k;
int main(){beta=2.961520e10; H=SPEEDC*SPEEDC*SPEEDC/beta;
M=1.9891E30; rs=6.95e8;rot=2*PI/(25.05*24*3600);v1=rot*rs;K1=v1*v1/2;//T1=2*PI*H/K1;
v2=0.7346*sqrt(BOLTZMANN*5700/MP)+0.2485*sqrt(BOLTZMANN*5700/(MP+MP));
K2=v2*v2/2;T2=2*PI*H/(K2-K1);T=T2/24*3600*365.2422;
Lamda=2*PI*H/(v2-v1);V=Lamda/T2;
SetViewAngle("temp0,theta60,phi-60");
DrawFrame(FRAME_LINE,1,0xafffaf);Overlook("2,1,60", D);
//TextAt(10,10,"v1=%d, v2=%d, T=%.2f y, λ=%e, V=%d",v1,v2,T, Lamda,V);
SetPen(1,0x4f4fff); for(i=0;i<18;i+=1) {v1=i*2*PI/18; x=70*cos(v1);y=70*sin(v1);Ring();}
SetPen(2,0xff0000);Draw("ARROW,0,2,XYZ,15","80,0,0,80,60,0");
TextHang(100,20,0,"top-layer ω#sd2#t"); SetPen(2,0x0000ff);
Draw("ARROW,0,2,XYZ,15","70,0,0,70,60,0");
TextHang(50,60,0,"center ω#sd1#t");TextHang(140,-30,0," ω#sdbeat#t=ω#sd2#t-ω#sd1#t");
}
Ring(){ k=0;N=20; r=10;
for(j=0;j<N+2;j+=1) {k=j+j+j; v2=j*2*PI/N;
D[k]=x+r*cos(v2);D[k+1]=y+r*sin(v2); D[k+2]=0;}
Plot("POLYLINE,4,22,XYZ,8",D);}
#v07=?>A#t
```

$$\psi = \psi_{top} + C\psi_{middle}$$

$$\psi_{top} = \exp[\frac{i\beta}{c^3}\int_L (v_1 dl + \frac{-c^2}{\sqrt{1-v_1^2/c^2}} dt)]$$

$$\psi_{middle} = \exp[\frac{i\beta}{c^3}\int_L (v_2 dl + \frac{-c^2}{\sqrt{1-v_2^2/c^2}} dt)]$$

(25)

Their interference in the coherent width direction leads to a beat phenomenon

$$|\psi|^2 = |\psi_{top} + C\psi_{middle}|^2 = 1 + C^2 + 2C\cos[\frac{2\pi}{\lambda_{beat}}\int_L dl - \frac{2\pi}{T_{beat}}t]$$

$$\frac{2\pi}{T_{beat}} = \frac{\beta}{c^3}(\frac{c^2}{\sqrt{1-v_1^2/c^2}} - \frac{c^2}{\sqrt{1-v_2^2/c^2}}) \simeq \frac{\beta}{c^3}(\frac{v_1^2}{2} - \frac{v_2^2}{2}) \qquad (26)$$

$$\frac{2\pi}{\lambda_{beat}} = \frac{\beta}{c^3}(v_1 - v_2); \quad V = \frac{\lambda_{beat}}{T_{beat}} = \frac{1}{2}(v_1 + v_2)$$

Their speeds are calculated by

$$v_1 \approx 6200\,(m/s) \quad (\approx \text{observed in Evershed flow})$$
$$v_2 = \omega r_{middle} = 2017\,(m/s) \quad (\text{sun rotation}); \qquad (27)$$

Where, regarding Evershed flow as the eruption of the top-layer flow, about 6km/s speed was reported [31]. Alternatively, the top-layer speed v_1 also can be calculated by thermodynamics, to be v_1=6244 (m/s) [28]. Thus, their beat period T_{beat} is calculated to be a very remarkable value of 10.38 (years), in agreement with the sunspot cycle value (say, mean 11 years).

$$T_{beat} \simeq \frac{4\pi c^3}{\beta(v_1^2 - v_2^2)} = 10.38\,(years)\,. \qquad (28)$$

The relative error to the mean 11 years is 5.6% for the beat period calculation using the acceleration-roll waves. This beat phenomenon turns out to be a nucleon density oscillation that undergoes to drive the sunspot cycle evolution. The beat wavelength λ_{beat} is too long to observe, only the beat period is easy to be observed. This nucleon density oscillation is understood as a new type of nuclear reaction on an astronomic scale.

In the above calculation, although this seems to be a rough model, there is an obvious correlation between solar radius, solar rotation, solar density, ultimate acceleration, and Planck-constant-like constant h.

8. Atmospheric circulation

Consider an acceleration-roll wave ψ_A in the earth shell at the latitude angle A, it will interfere with its neighbor waves within its coherent width. Because the earth shell mainly consists of dense matter, their mutual cascade-interference will cause the acceleration roll wave to have the same phase at the same longitude, so that the acceleration roll wave ψ_A should equal to the $\psi_{equator}$ at the same longitude, as shown in Fig.10(a). This conclusion is supported by the spherical symmetry of the Earth's density distribution, that is.

$$\text{spherical symmetry: } \rho(r, A, \varphi) = \rho(r) \implies \psi(r, A, \varphi) = \psi(r)$$
$$\text{or: } \psi_A = \psi_{equator} \qquad (29)$$

On the contrary, in the thin atmosphere, the cascade-interference within the coherence width can be ignored, so the wind and clouds are widely distributed in the sky on a large scale.
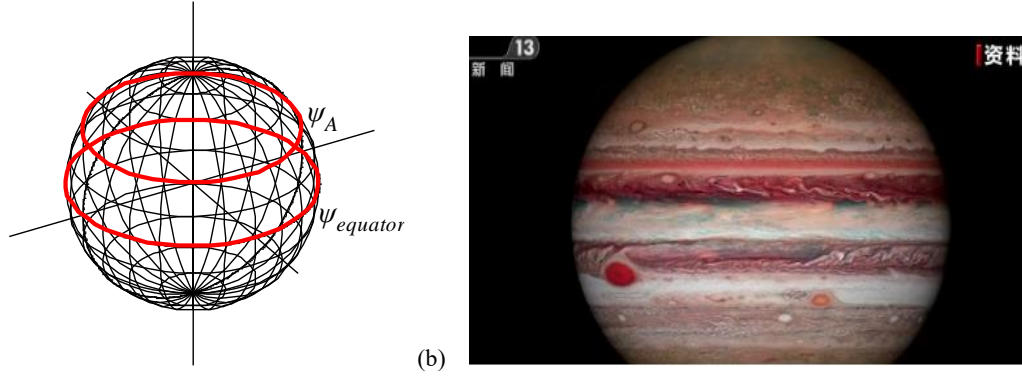
Fig.10   (a) Mutual cascade-interference will lead to the acceleration-roll wave having the same phase. (b) Jupiter (the photo from News).

```
<Clet2020 Script>// [26]
double beta,H,M,dP[20],D[2000],r,rs,rot,x,y,v1,v2,K1,K2,T1,T2,T,Lamda,V; int i,j,k,N;
int main(){beta=2.961520e10; H=SPEEDC*SPEEDC*SPEEDC/beta;
M=1.9891E30; rs=6.95e8;rot=2*PI/(25.05*24*3600);v1=rot*rs;K1=v1*v1/2;//T1=2*PI*H/K1;
v2=0.7346*sqrt(BOLTZMANN*5700/MP)+0.2485*sqrt(BOLTZMANN*5700/(MP+MP));
K2=v2*v2/2;T2=2*PI*H/(K2-K1);T=T2/24*3600*365.2422;
Lamda=2*PI*H/(v2-v1);V=Lamda/T2;
SetViewAngle("temp0,theta60,phi-60");
DrawFrame(FRAME_LINE,1,0xafffaf);Overlook("2,1,60", D);
for(i=0;i<180;i+=15) {k=0; K1=0; K2=i;Grid();}
for(i=0;i<180;i+=15) {k=1; K1=i; K2=0;Grid();}
//TextAt(10,10,"v1=%d, v2=%d, T=%.2f y, λ=%e, V=%d",v1,v2,T, Lamda,V);
SetPen(3,0xff0000); k=1; K1=60; K2=0;Grid();K1=90; K2=0; Grid();
//SetPen(3,0x4f4fff); k=1; K1=55; K2=0;Grid();K1=65; K2=0; Grid();
TextHang(40,40,50,"#ifψ#sdA#t"); TextHang(50,40,0,"#ifψ#sdequator#t");
}
Grid(){N=50; K1*=PI/180; K2*=PI/180;   r=60;
if(k==0) {v1=2*PI/N; v2=0;} else {v1=0; v2=2*PI/N;}
for(j=0;j<=N;j+=1){ k=j+j+j;
D[k]=r*sin(K1)*cos(K2);D[k+1]=r*sin(K1)*sin(K2); D[k+2]=r*cos(K1);
K1+=v1;K2+=v2; }Plot("POLYGON,0,50, XYZ,10",D);
}#v07=?>A#t
```

Through the coherent width concept, considering the interference between the air ψ_A at the latitude angle A and the shell ψ_{shell} at the same latitude, they are

$$\psi(r,A) = \psi_{air}(r,A) + C\psi_{shell}(r,A) = \psi_{air}(r,A) + C\psi_{shell\_equator}(r)$$

$$T_{beat} \simeq \frac{4\pi c^3}{\beta\left(v_{shell\_equator}^2 - v_{air}^2\right)}$$. (30)

$$v_{shell\_equator} = \omega r$$

$$v_{air} = \omega r \cos(A) + v_{wind} + v_{sun\_effect}$$

where C represents the coupling constant which relates to their distance and mass fractions, their interference leads to a beat phenomenon. The positive wind denotes the direction from west to east. The air subjects to the solar radiation which enforces the beat oscillation to run at the period T_{beat}=1 (year) at the latitude angles A=-23.5°N ~ 23.5°N due to the tilt of the earth axis concerning the earth orbital plane. In the northern hemisphere the sun mainly shines the earth surface at the mean latitude angle A=12°N, so we focus on the latitude A=12°N location where the constructive interference condition is supposed to be satisfied with a wind speed of zero, thus the beat formula is used to determine that v_{sun_effect} =-85(m/s) at the mostly shined latitude. Covering all shined latitudes, we finally decide

$$v_{sun\_effect} = -85\cos(A-12°) \quad (m/s) \ .$$ (31)

Near the latitude A=12°N location, it is not easy to maintain the constructive interference condition

for these waves. The wind required for maintaining the beat T_{beat}=1 (year) near the latitude A=12°N is calculated as shown in Fig.11(a) (blue line), this wind will be destroyed by destructive interference waves at higher latitudes. But, the wind will arise up again at the next locations where the waves satisfy the constructive interference condition: at A=48°N location where beat T_{beat}=0.5 (years), and at A=77°N location where beat T_{beat}=0.37 (years) which is the shortest period that the earth can get within the arctic regions. Linking all characteristic points in Fig.11(a) we obtain the predicted wind-curve over the northern hemisphere; this prediction agrees well with the experimental observations at an altitude of 10km (200hPa), as shown in Fig.12.
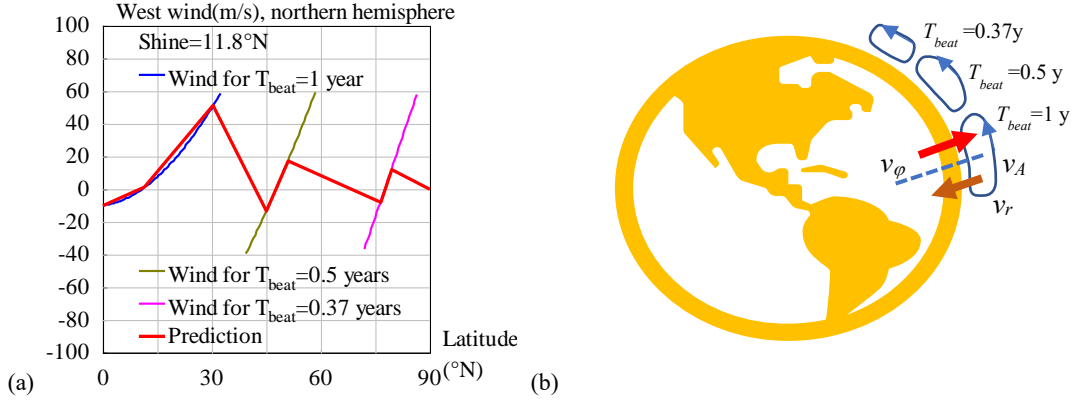

Fig.11 (a) Calculation of west winds in the northern hemisphere. (b) The atmospheric circulation in the northern hemisphere.

```
<Clet2020 Script>// [26]
double beta,H,M,r,rc, rs,rot,v1,v2, Year,T,A,B,Lamda,V,a,b,w,N[500],S[500],F[100]; int i, j, k,   m, n, s, f, f1,F1,f2,F2,Type,x;
int main(){beta=1.377075e+14; H=SPEEDC*SPEEDC*SPEEDC/beta;
M=5.97237e24; rs=6.371e6; rot=2*PI/(24*3600); Year=24*3600*365.2422;
Type=1; x=10; if(Type>1) x=-30;
if(Type==1)   SetAxis(X_AXIS,0,0,90,"Latitude#n(°N);0;30;60;90;");
else   SetAxis(X_AXIS,-90,-90,90,"Latitude#n(°N);=90;-60;-30;0;30;60;90;");
SetAxis(Y_AXIS,-100,-100,100,"West wind(m/s), northern hemisphere;-100;-80;-60;-40;-20;0;20;40;60;80;100;");
DrawFrame(0x016a,Type,0xafffaf);//Polyline(2,"-90,0,90,0");
A=30; Check(15,k); if(k>24) k=24; if(k<0) k=0; B=-23.5+47*k/24; j=180; f=0;
T=Year; F1=0;F2=50; Wind();
SetPen(2,0xff); Polyline(n,N,x,70,"Wind for T#sdbeat#t=1 year"); if(Type>1) Polyline(s,S);
F[0]=N[0];F[1]=N[1]; F[2]=N[f1+f1]; F[3]=N[f1+f1+1];   F[4]=N[f2+f2]; F[5]=N[f2+f2+1];
T=Year/2;   F1=-15; F2=15; Wind();
SetPen(2,0x80ff00); Polyline(n,N,x,-50,"Wind for T#sdbeat#t=0.5 years"); if(Type>1) Polyline(s,S);
F[6]=N[f1+f1]; F[7]=N[f1+f1+1];   F[8]=N[f2+f2]; F[9]=N[f2+f2+1];
T=0.37*Year;   F1=-10; F2=10; Wind();
SetPen(2,0x9933fa); Polyline(n,N,x,-70,"Wind for T#sdbeat#t=0.37 years"); if(Type>1) Polyline(s,S);
F[10]=N[f1+f1]; F[11]=N[f1+f1+1];   F[12]=N[f2+f2]; F[13]=N[f2+f2+1];   F[14]=90; F[15]=0;
SetPen(3,0xff0000); Polyline(8,F,x,-90,"Prediction");
TextHang(x,90,0,"Shine=%.1f°N", B);
}
Wind(){//T, B,
n=0;s=0; f1=0;f2=0;
for(i=0;i<180;i+=1)   { a=i*PI/360;b=(i/2-B)*PI/180;w=-85*cos(b);
v1=rot*rs*cos(a); v2=rot*rs; a=v2*v2/2-2*PI*H/T; V=sqrt(a+a)-v1-w;
if(V>F1 && f1==0) f1=n;if(V>F2 && f2==0) f2=n;
if(V>-40 && V<60) {N[n+n]=i/2; N[n+n+1]=V; n+=1;}}
for(i=0;i<180;i+=1)   { a=-i*PI/360;b=(-i/2-B)*PI/180;w=-85*cos(b);
v1=rot*rs*cos(a); v2=rot*rs; a=v2*v2/2-2*PI*H/T; V=sqrt(a+a)-v1-w;
if(V>-40 && V<60) {S[s+s]=-i/2; S[s+s+1]=V; s+=1;} }
}}
#v07=?>A#t
```

For further improvement of precision, the wind required by the constructive interference condition should be understood as a magnitude, it can be resolved into three components in the spherical coordinates (r, A, φ) as

$$v_{wind}{}^2 = v_r{}^2 + v_A{}^2 + v_\varphi{}^2 . \tag{32}$$

According to the energy equipartition theorem in thermodynamics, approximately we have the

average estimation

$$< v_r^2 > = < v_A^2 > = < v_\varphi^2 > = \frac{1}{3} v_{wind}^2 \quad . \tag{33}$$

Thus, the wind vectors around the northern hemisphere of the Earth are plotted in Fig.11(b), the atmospheric circulation consists of three cells: Hadley cell, Ferrel cell, and arctic cell.
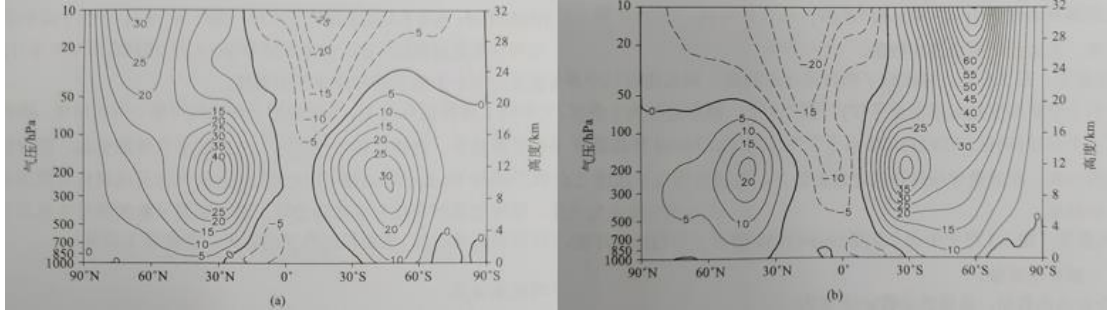

Fig.12   NCEP/NCAR data, mean west winds over 40 years (1958~1997) [36]. (a) in winter; (b) in summer.

The beat T_{beat}=0.5 (years) blows comfortable winds over Europe, Northern America and Northeastern Asia, and modulates the four seasons; the shortest beat T_{beat}=0.37 (years) has a beat wavelength too long to be confined in the arctic regions so that it escapes from the north pole toward the equator, so recognized as the planet-scale waves or Rossby waves.

Since the acceleration-roll wave of the air interferes with the acceleration-roll wave of the equatorial shell, the easterlies at the equator have a magnitude of about 10 m/s. The trade winds or easterlies are the permanent east-to-west prevailing winds that flow in the Earth's equatorial region. The trade winds blow mainly from the northeast in the Northern Hemisphere and the southeast in the Southern Hemisphere, strengthening during the winter and when the Arctic oscillation is in its warm phase. Trade winds have been used by captains of sailing ships to cross the world's oceans for centuries. The driving force of atmospheric circulation is the uneven distribution of solar heating across the earth, which is greatest near the equator and least at the poles. This air rises to the tropopause, about 10–15 kilometers above sea level, where the air is no longer buoyant [33].

Consider a funny issue, as we have known that v_{sun_effect} =-85(m/s) at the equator, imagine if nuclear wars happen on the Earth to stop the solar radiation to the Earth's surface, then the equatorial wind on the Earth's surface will simply reach to 95 (m/s), like the winds on the surfaces of the Jupiter and Saturn [28], this will change global climate mode, killed all dinosaurs by strong winds and dusts. Thinking about Mars, Jupiter, and Saturn that gain very weak solar radiation, and there are at least 100 (m/s) strong winds on their surfaces, as shown in Fig.10(b). It tells us how important is the easterly 10 (m/s) at the equator for us, and how important is the air pollution for us. Have you ever gotten an experience: the more serious the air pollution, the stronger the wind? This section helps us understand how the dinosaurs to be buried.

9.   Inner structure of tropical cyclones

A tropical cyclone is a rapidly rotating storm system characterized by a low-pressure center, a closed low-level atmospheric circulation, strong winds, and a spiral arrangement of thunderstorms that produce heavy rain and squalls. Tropical cyclones on either side of the Equator generally have their origins in several tropical cyclone basins, as shown in Fig.13. The Northwest Pacific Ocean is the

most active basin on the planet, accounting for one-third of all tropical cyclone activity. Warm sea surface temperatures are required for tropical cyclones to form and strengthen. The commonly-accepted minimum temperature range for this to occur is 26–27 °C [37,38].

(a)   (b)
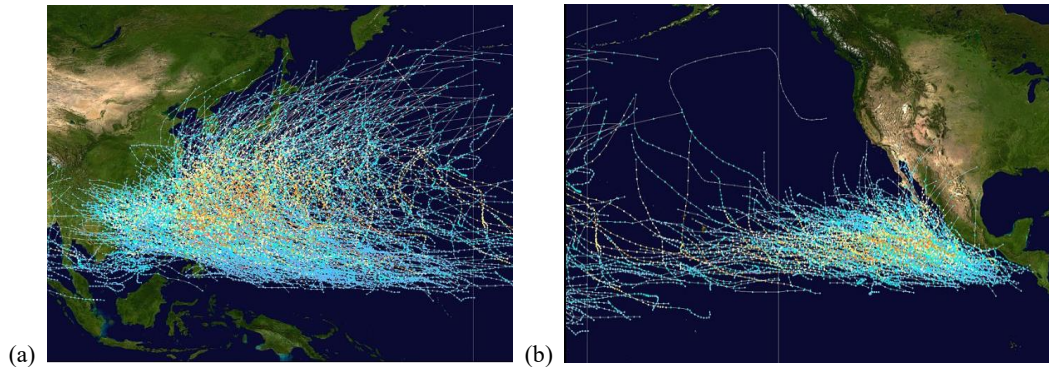
Fig.13   (a) Tracks of all tropical cyclones in the northwestern Pacific Ocean between 1980 and 2005.[39]. (b) Tracks of all tropical cyclones in the northern Pacific Ocean east of the International Date Line between 1980 and 2005.[39]

The latitude A=12°N is called the first constructive interference ridge sandwiched between easterlies and westerlies, where the shear action of the winds will produce a lot of vortexes if the winds are disturbed by vapors at higher altitudes. The pregnancy of a tropical cyclone needs three steps, as shown in Fig.14(a).
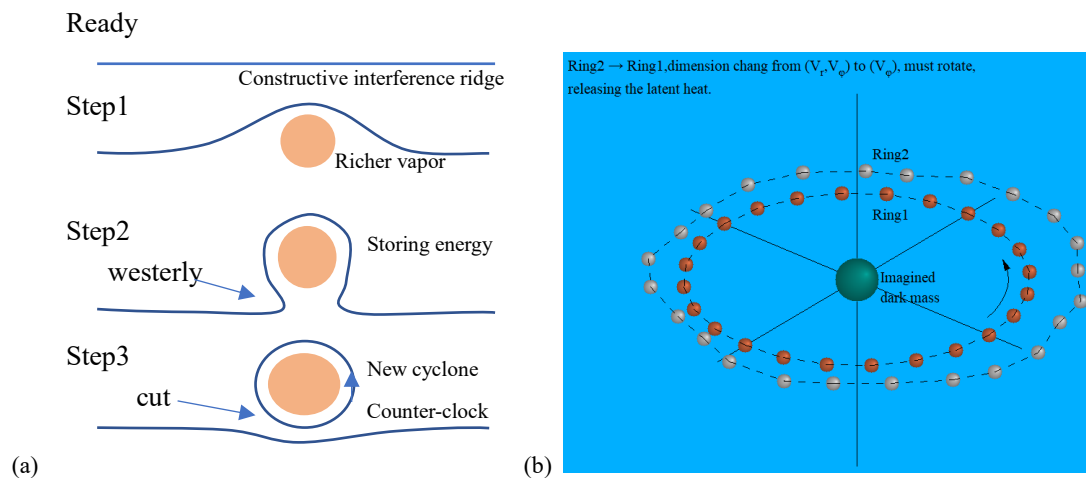

(a)   (b)

Fig.14   (a)Three steps of the pregnancy of a tropic cyclone in the northern hemisphere. (b) Dimension change on a molecular scale.

```
<Clet2020 Script>// [26]
double r,x,y,z,v, a,b,c,dP[20],D[500];    int i,j,k ;
main(){ SetViewAngle("temp0,theta60,phi-40"); DrawFrame(FRAME_LINE,2,0xafff);
dP[0]=PEARL; dP[1]=0xefefef; dP[2]=1; dP[3]=XYZ;
dP[4]=10; dP[5]=10; dP[6]=0; dP[7]=50; dP[8]=30; dP[9]=30;
r=100; b=10; j=0;
for(i=0;i<360;i+=15) { a=i*PI/180; x=r*cos(a); y=r*sin(a); z=0;
x+=b*random(); y+=b*random();
D[j+j+j]=x; D[j+j+j+1]=y; D[j+j+j+2]=z; Plot(dP,D[j+j+j]); j+=1;}
Plot("POLYGON,1,@j,XYZ,10,",D);
r=80; b=6; dP[1]=0xff7f50; j=0;
for(i=0;i<360;i+=15) { a=i*PI/180; x=r*cos(a); y=r*sin(a); z=0;
D[j+j+j]=x; D[j+j+j+1]=y; D[j+j+j+2]=z; Plot(dP,D[j+j+j]); j+=1;}
Plot("POLYGON,1,@j,XYZ,10,",D);
TextHang(10,0,70,"Ring2#n#n#nRing1");
TextAt(100,200,"Ring2 →  Ring1,dimension chang from (V#sdr#t,V#sdφ#t) to (V#sdφ#t), must rotate,#nreleasing the latent heat.");
D[0]=0; D[1]=0; D[2]=0; dP[1]=0x03a89e; dP[4]=30; dP[5]=30; Plot(dP,D);
```

18

TextHang(8,8,0,"Imagined #ndark mass"); r=70;   j=0;
for(i=10;i<60;i+=5) { a=i*PI/180; x=r*cos(a); y=r*sin(a); z=0;
D[j+j+j]=x; D[j+j+j+1]=y; D[j+j+j+2]=z; j+=1;}
dP[0]=POLYLINE; dP[1]=3; dP[2]=j; dP[3]=XYZ; dP[4]=15; Plot(dP,D);
}
#v07=?>A#t

Step1, during summer, the richer vapor at higher altitudes over the warm sea surface dramatically absorbs the solar radiation and releases the v_{sun_effect} =-85(m/s) into the air at lower altitudes; consequently, the strengthened easterlies make a distortion to the first constructive interference ridge, as shown in Fig.14(a).

Step2, day by day, the distortion develops to an extent that it is going to separate from the mother-like first constructive interference ridge hit strongly by the westerlies, as shown in Fig.14(a).

Step3, finally, the distorted constructive interference ridge grows up to become an isolated baby ring which is recognized as a new tropical cyclone, counter-clockwise in the northern hemisphere, as shown in Fig.14(a), similar to Fig.10(b) there is a large vortex on the surface of Jupiter.

The pregnancy of tropical cyclones tends to develop at the latitude A=12°N, it is a relativistic quantum mechanical effect that cannot be solved by classical fluid mechanics. Recalling that the latitude A=12°N represents the mean latitude angle which subjects to the main solar radiation activity in the northern hemisphere, actually, the solar radiation varies its mostly shined latitudes within the range of A=-23.5°N ~ 23.5°N due to the tilt of the earth axis concerning the earth orbital plan, therefore actual pregnancy latitude of tropical cyclones occur among latitude angles A=-23.5°N ~ 23.5°N, this result agrees well with the experimental records.

In Fig.11(a), there are the second, the third, …, constructive interference ridges to bear the pregnancy of cyclones, hurricanes, typhoons, storms, tornados. Without these flexible constructive interference ridges, it is difficult for classical physics to say that some disturbances would somehow support the persistence of the vortexes.

For understanding the pregnancy process on a molecular scale, considering there are two molecular rings in Fig.14(b), typically the air molecules move on the Earth's surface in 2D motion. From ring2 to ring1, there is a dimension change for the molecules whose velocity changes from (v_r,v_φ) to (v_φ), from 2D to 1D, losing the r component velocity. According to the energy equipartition theorem, every molecule would lose its kinetic energy as the latent heat released into the sky as

$$E_{latent} = \frac{2}{2}kT - \frac{1}{2}kT = \frac{1}{2}kT \quad .$$ (34)

At this moment, the molecules have to rotate about the cyclone's center. Losing an amount of the molecular kinetic energy will lead to the ring1 to be in a stationary bound state, whose binding force and binding energy are given by

$$F_{centripetal} = -\frac{\Delta E}{\Delta r} = -\frac{N_{molecules}E_{latent}}{\Delta r} \quad .$$ (35)

$$E_{binding} = N_{molecules}E_{latent}$$

As you wish, you can say that at the cyclone's center there exists an **imagined dark mass** which contributes to this binding force by using the universal gravitational formula.

When the constructive interference ring of a newly born cyclone forms, its wavelength will adapt to the ring size as

$$\frac{1}{hM_{cyclone}}\oint_L v_l dl = 2\pi n; \quad n = 1, 2, \ldots$$

$$\psi = \exp(\frac{i}{hM_{cyclone}}\int_0^x (u_1 dx_1 + u_2 dx_2 + u_3 dx_3 + u_4 dx_4))$$

(36)

where the mass M represents the overall mass of the new cyclone, including the **imagined dark mass** which accounts for the latent heat released during its formation; the constant h is the **Planck-constant-like constant** determined by experimental observations. The air molecules of the ring are under the control of their acceleration-roll waves whose coherent length is so long that the waves have to overlap as

$$\psi(r) = 1 + e^{i\delta} + e^{i2\delta} + \ldots + e^{i(N-1)\delta} = \frac{1 - \exp(iN\delta)}{1 - \exp(i\delta)}$$

$$\delta(r) = \frac{1}{hM_{cyclone}}\oint_L (v_l)dl$$

(37)

This formula can be used to calculate the distribution of the cyclone's nucleon density. In the preceding section on the central state optical model, we have mentioned that the air-vapor only concerns one wavelet interference, so that the overlapping number N of air-vapor of the cyclones simply takes 2, the structure of tropical cyclones becomes easier to calculate, that is

$$\psi(r) = 1 + e^{i\delta} = 1 + \cos(\delta) + i\sin(\delta) .$$

(38)

It follows that the full expression is given in 2D cylinder wave form by

$$\psi(r)_{interference} = \sqrt{\frac{r_0}{r}}\sin(\delta)e^{i(k_r r - \omega t)} = \sqrt{\frac{r_0}{r}}\sin(\frac{v2\pi r}{hM})e^{i(k_r r - \omega t)} .$$

(39)

On an altitude scale, a cyclone is divided into two layers: the upper layer and the lower layer. In the lower layer at the first ring the radius r_0 is proportional to the wavelength λ of the acceleration-roll wave, the swirling wind speed approximately is inversely proportional to radius r, and the maximal speed is about 45 (m/s) according to the theoretical prediction of the maximal wind in Fig.11(a) and the experimental observations in Fig.15(a), then
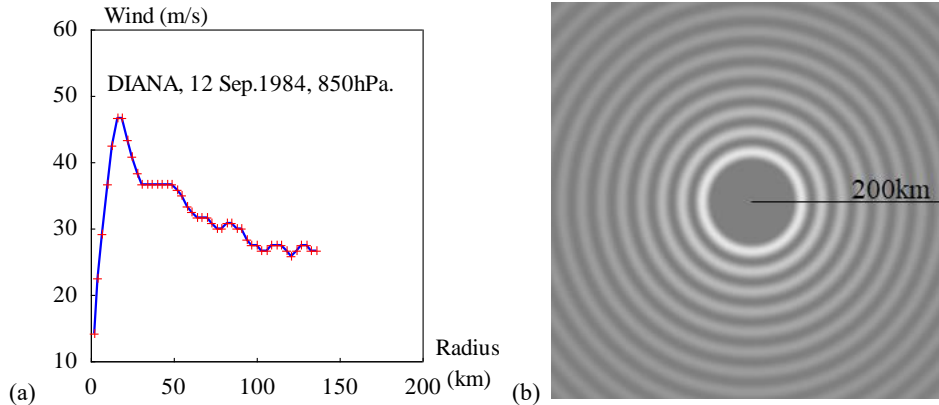

Fig,15   (a)Gradient wind as a function of the radius for the hurricane DIANA (12, Sep.1984) measured at 850hPa [40]. (b) The simulation of a cyclone using acceleration-roll wave, |x|<200km.

<Clet2020 Script>//[26]
int i,j,k,n; double x,y,nP[10];
int
D_Wind[92]={2,5,4,15,7,23,10,32,13,39,16,44,19,44,22,40,25,37,28,34,31,32,34,32,37,32,40,32,43,32,46,32,49,32,52,31,55,30,
58,28,61,27,64,26,67,26,70,26,73,25,76,24,79,24,82,25,85,25,88,24,91,24,94,22,97,21,100,21,103,20,106,20,109,21,112,21,115,

20

21,118,20,121,19,124,20,127,21,130,21,133,20,136,20,};
main(){SetAxis(X_AXIS,0,0,200,"Radius#n   (km);0;50;100;150;200;");
SetAxis(Y_AXIS,0,0,60,"Wind (m/s); 10;20;30;40;50;60;");
DrawFrame(FRAME_BOX,1,0xafffaf); j=46;
SetPen(2,0xff); Polyline(j,D_Wind); SetPen(1,0xff0000);
nP[0]=CROSS;nP[1]=0;nP[2]=j;nP[3]=XY;nP[4]=4;nP[5]=4;Plot(nP,D_Wind);
TextHang(10,50,0,"DIANA, 12 Sep.1984, 850hPa.");
}#v07=?>A#t

<Clet2020 Script>//[26]
int i,j,k,nP[10]; double r_unit,Lamda,r,r0,r1,r2,v,v0,v1,w, a,b,delta, D[100];//1D array
main(){ w=150; r_unit=1e3;//km
r0=30*r_unit; r1=r0; Lamda=2*PI*r0; v0=15;v1=30;//m/s
DrawFrame(FRAME_NULL,1,0xafffaf); nP[0]=SET; nP[1]=1; nP[2]=PX;
for(i=-w;i<w;i+=1) { for(j=-w;j<w;j+=1) { r2=i*i+j*j;r=sqrt(r2)*r_unit;
if(r>r0)   {b=r0/r; v=v0+v1*b; } else {b= 0; v=v0*b;}
delta=2*PI*v*2*PI*r/(v0*Lamda);
a=sin(delta); a*=a; a*=b;//2D cylinder wave attenuation
nP[3]=Colorize(1,0xffffff,a);D[0]=250+i;D[1]=250+j;D[2]=0;PixelJob(nP,D); }}
Draw("LINE,0,2,XY,10","0,0,100,0");TextHang(50,5,0,"200km");
}#v07=?>A#t

$$2\pi r_0 = \lambda; \quad v_r = \frac{hM}{2\pi} k_r$$

(40)

$$r > r_0: \quad v_\varphi = v_0 + v_1 \frac{r_0}{r}; \quad v_0 = 15(m/s); \quad v_1 = 30(m/s)$$

A cyclone's acceleration-roll wave interference is simulated as shown in Fig.15(b), clearly showing the inner structure of a cyclone, well compared with the DIANA cyclone on 12 Sep. 1984 in situ observation measured by an aircraft [40]. Don't underestimate the profound role of the Planck-constant-like constant in cyclone structure; without it, all return to the classical fluid mechanics.

What is dark matter? Why it is important for cyclones and galaxies? Consider a galaxy whose gravity can captures any stars near the galaxy center by the universal gravitational force; the near field of the gravity can capture any star strolling in the galaxy's 2D plane and finally let this star move in a 1D circular orbit approximately, it makes a dimension change for the star from 2D to 1D with releasing latent heat. The far field of the gravity has to face stars strolling in 3D space, if it wants to capture these far stars, it must have an ability stronger than the universal gravitational force; in the far field, the gravitational force must become to be proportional to $1/r$, which thus can capture far stars by releasing more latent heat in comparison to capturing near stars. Therefore, the gravitational force of the galaxy should be modified as

$$f = a\frac{GM}{r} + m\frac{GM}{r^2} = \begin{cases} m\dfrac{GM}{r^2} & near\_field : \text{capturing 2D to1D} \\ a\dfrac{GM}{r} & far\_field : \text{capturing 3D to1D} \end{cases}$$

(41)

where the coefficient a only works in the far field of the gravity of the galaxy. In the viewpoint of the classical universal gravitational force, the far field attributes more unseen mass to the gravity effect, the unseen mass is recognized as the dark matter of the galaxy.

10. Why dimension change causes spin

Dimension is defined as the number of independent parameters in a mathematical space. In the field

of physics, dimension is defined as the number of independent space-time coordinates. 0D is an infinitesimal point with no length. 1D is an infinite line, only length. 2D is a plane, which is composed of length and width. 3D is 2D plus height component, has volume.

In this section, we at first discuss how to measure dimension by a wave. In Fig.16(a), one puts earphones into ear, one gets a 1D wave in the ear tunnel.

$$1D: \quad y = A\sin(kr - \omega t) = \frac{A}{r^0}\sin(kr - \omega t) \cdot \tag{42}$$

where r is the distance between the wave emitter and the receiver. In Fig.16(b), if one touches a guitar spring, one gets a 2D cylinder wave.

$$2D: \quad y = \frac{A}{r^{1/2}}\sin(kr - \omega t) \cdot \tag{43}$$

In Fig.16(c), one turns on a music speaker, one gets a 3D spherical wave.

$$3D: \quad y = \frac{A}{r}\sin(kr - \omega t) \cdot \tag{44}$$

(a) 1D tunnel wave   (b) 2D cylinder wave   (c) 3D spherical wave
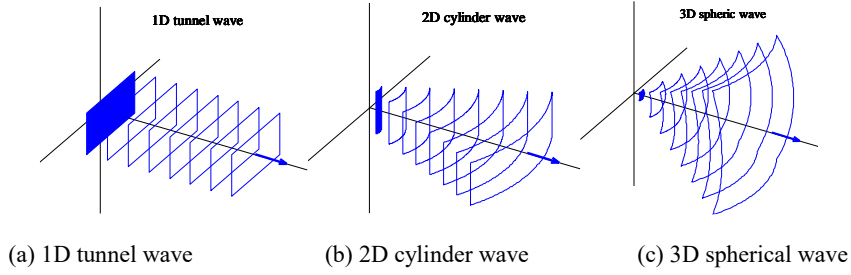
Fig.16   The wave behavior in various dimensional spaces.

```
<Clet2020 Script>// Clet is a C compiler [26]
int i,j,k,type,nP[10]; double D[20],S[1000];
int main(){SetViewAngle("temp0,theta60,phi-30");SetAxis(X_AXIS,0,0,200,"X;0;200;");
DrawFrame(FRAME_LINE,1,0xafffaf); type=2;SetPen(1,0x00ff);
for(i=10;i<160;i+=20){D[0]=i;D[1]=0;D[2]=0;D[3]=i+5;D[4]=0;D[5]=0;D[6]=i;D[7]=10;D[8]=0;
if(type==0) {D[9]=4;D[10]=40;D[11]=20;D[12]=i;TextHang(50,0,100,"1D tunnel wave");k=CARD;}
else if(type==1) {D[9]=200;D[10]=i/2;D[11]=20;D[12]=i;TextHang(50,0,100,"2D cylinder wave");k=50;}
else {D[9]=200;D[10]=i/2;D[11]=i/2;D[12]=i;TextHang(50,0,100,"3D spheric wave");k=40;}
Lattice(k,D,S);nP[0]=POLYGON;nP[1]=0;nP[2]=200;nP[3]=XYZ;
if(i==10) nP[1]=3; if(type==0) nP[2]=4; Plot(nP,S[9]);}
j=30;D[3]=D[0]+j*S[0];D[4]=D[1]+j*S[1];D[5]=D[2]+j*S[2];
SetPen(3,0x00ff);Draw("ARROW,0,2,XYZ,10",D);}}
#v07=?>A#t
```

In general, we can write a wave in the form

$$y = \frac{A}{r^w}\sin(kr - \omega t) \cdot \tag{45}$$

It is easy to get the dimension of the space in where the wave lives, the dimension is $D=2w+1$. Nevertheless, the wave can be used to measure the dimension of space, just by determining the parameter w.

Waves all contain a core oscillation (vibration invariance. Hubble's law not only tells us about redshift, but also clarifies the real situation in a sense: vibration invariance.)

$$\frac{d^2y}{dr^2} + k^2y = 0, \tag{46}$$

Substituting y into the core oscillation, we obtain the radial wave equation

$$\frac{d^2y}{dr^2} + \frac{2w}{r}\frac{dy}{dr} + (k^2 + \frac{w(w-1)}{r^2})y = 0 \cdot \tag{47}$$

22

This equation expresses the wave behavior modulated by the spatial dimension parameter w. For 1D wave $w=0$, it is trivial, but for 2D wave $w=1/2$, it reduces to the Bessel equation in a cylinder coordinate system (r,φ)

$$\frac{d^2y}{dr^2}+\frac{1}{r}\frac{dy}{dr}+(k^2-\frac{1}{4r^2})y=0 \quad \text{(2D wave)}$$

comparing to the Schrodinger's equation: · (48)

$$\frac{d^2R(r)}{dr^2}+\frac{2}{r}\frac{dR(r)}{dr}+[k^2-\frac{l(l+1)}{r^2}]R(r)=0$$

In quantum mechanics, y is an electronic wave function, comparing to the Schrodinger radial wave equation in textbooks, we find that the $-1/4r^2$ term represents the electronic spin effect. However, here according to the above radial Bessel equation, we can simply conclude that sound waves, electromagnetic waves, or any wave can have a spin effect in 2D space! Let us use $\boldsymbol{k}$ to denote the wave-vector, then the above 2D wave equation tells us

$$k_r^2=k^2-k_\varphi^2; \quad k=\frac{2\pi}{\lambda}; \quad k_\varphi=\pm\frac{1}{2r}· \tag{49}$$

The k_φ causes the 2D wave-vector $\boldsymbol{k}$ to spin little by little as illustrated in Fig.17. The positive and negative k_φ corresponds to spin up and spin down respectively; as r goes to infinity, the spin effect vanishes off.
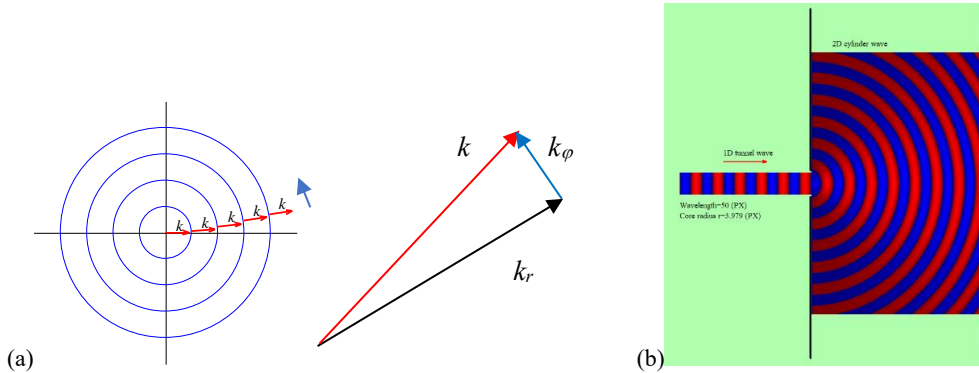

Fig.17   (a) 2D wave-vector k spins little by little in the cylinder coordinates (r,φ). (b) from 1D to 2D, the spin works to split the electron beam due to the double-value k_φ.

```
<Clet2020 Script>// Clet is a C compiler [26]
int i,j,k;double r,x,y,a,D[100];
int main(){DrawFrame(FRAME_LINE,1,0xafffaf); SetPen(1,0x0000ff);
for(i=0;i<90;i+=20) {D[0]=-i;D[1]=-i;D[2]=i;D[3]=i; Draw("ELLIPSE,0,2,XY,0",D);}
for(i=0;i<90;i+=20) {a=0.2*(i-i*i/200)*PI/180;r=i;D[0]=r*cos(a);D[1]=r*sin(a);
r+=18;D[2]=r*cos(a);D[3]=r*sin(a); SetPen(2,0xff0000);
Draw("ARROW,0,2,XY,8",D);TextHang(D[2]-10,D[3]+5,0,"#ifk");}
}#v07=?>A#t
```

If the 2D wave is the de Broglie matter wave for a particle beam, in a cylinder coordinate (r,φ), then the matter wave has a spin angular momentum J given by

$$k_r=\frac{p_r}{\hbar}; \quad k_\varphi=\frac{p_\varphi}{\hbar}=\frac{J_\varphi}{r\hbar}; \quad J_\varphi=\pm\frac{1}{2}\hbar· \tag{50}$$

According to the angular momentum formula in general physics, it is recognized that the particle total momentum p is a constant given by

$$\left(\frac{p}{\hbar}\right)^2 = \left(\frac{p_r}{\hbar}\right)^2 + \left(\frac{p_\varphi}{\hbar}\right)^2 .$$

$$k^2 = k_r{}^2 + k_\varphi{}^2 = const. \tag{51}$$

Since the particle total wave vector k is a constant, the wave-vector k_r must vary as r changes. The wave-vector in the radial direction would change as the wave attenuates.

Appling the spin to tropic cyclones, the swirling speed including the spin speed and earth's self-rotation effect, etc., is simply given by

$$v = v_0 + v_1 \frac{r_0}{r} . \tag{52}$$

That is what was observed.

11. Conclusions

In analogy with the ultimate speed c, there is an ultimate acceleration β, nobody's acceleration can exceed this limit β, in the solar system, β=2.961520e+10(m/s^2). Because this ultimate acceleration is large, any effect related to β will become easy to test, including quantum gravity tests. In this paper, an approach is put forward to connect the ultimate acceleration with quantum theory, as an application, this relativistic model gives out the sunspot cycle to be 10.38 years due to the ultimate acceleration. The same approach is applied to tropic cyclone problems, the simulation was carried out, clearly showing the inner structure of a cyclone, which is very consistent with the famous DIANA cyclone on 12 September 1984 in situ observation measured by an aircraft.

References
[1]C. Marletto, and V. Vedral, Gravitationally Induced Entanglement between Two Massive Particles is Sufficient Evidence of Quantum Effects in Gravity, Phys. Rev. Lett., 119, 240402 (2017)
[2]T. Guerreiro, Quantum effects in gravity waves, Classical and Quantum Gravity, 37 (2020) 155001 (13pp).
[3]S. Carlip, D. Chiou, W. Ni, R. Woodard, Quantum Gravity: A Brief History of Ideas and Some Prospects, International Journal of Modern Physics D, V,24,14,2015,1530028. DOI:10.1142/S0218271815300281.
[4]de Broglie, L., CRAS,175(1922):811-813, translated in 2012 by H. C. Shen in Selected works of de Broglie.
[5]de Broglie, Waves and quanta, Nature, 112, 2815(1923): 540.
[6]de Broglie, Recherches sur la théorie des Quanta, translated in 2004 by A. F. Kracklauer as De Broglie, Louis, On the Theory of Quanta. 1925.
[7]NASA, https://solarscience.msfc.nasa.gov/interior.shtml.
[8]NASA, https://nssdc.gsfc.nasa.gov/planetary/factsheet/marsfact.html.
[9]B. Ryden Introduction to Cosmology, Cambridge University Press, 2019, 2nd edition.
[10]D. Valencia, D. D. Sasselov,R. J. O'Connell, Radius and structure models of the first super-earth planet, The Astrophysical Journal, 656:545-551, 2007, February 10.
[11]D. Valencia, D. D. Sasselov,R. J. O'Connell, Detailed models of super-earths: how well can we infer bulk properties? The Astrophysical Journal, 665:1413–1420, 2007 August 20.
[12]T. Guillot, A. P. Showman, Evolution of "51Pegasusb-like" planets, Astronomy & Astrophysics,2002, 385,156-165, DOI: 10.1051/0004-6361:20011624
[13]T. Guillot, A. P. Showman, Atmospheric circulation and tides of "51Pegasusb-like" planets, Astronomy & Astrophysics,2002, 385,166-180, DOI: 10.1051/0004-6361:20020101
[14]L.N. Fletcher,Y.Kaspi,T. Guillot, A.P. Showman, How Well Do We Understand the Belt/Zone Circulation of Giant Planet Atmospheres? Space Sci Rev, 2020,216:30. https://doi.org/10.1007/s11214-019-0631-9
[15]Y. Kaspi, E. Galanti, A.P. Showman, D. J. Stevenson, T. Guillot, L. Iess, S.J. Bolton, Comparison of the Deep Atmospheric Dynamics of Jupiter and Saturn in Light of the Juno and Cassini Gravity Measurements,Space Sci Rev, 2020, 216:84. https://doi.org/10.1007/s11214-020-00705-7
[16]Orbital Debris Program Office, HISTORY OF ON-ORBIT SATELLITE FRAGMENTATIONS, National Aeronautics and Space Administration, 2018, 15 th Edition.
[17]M. Mulrooney, The NASA Liquid Mirror Telescope, Orbital Debris Quarterly News, 2007, April,v11i2,
[18]Orbital Debris Program Office, Chinese Anti-satellite Test Creates Most Severe Orbital Debris Cloud in History, Orbital Debris Quarterly News, 2007, April,v11i2,
[19]A. MANIS, M. MATNEY, A.VAVRIN, D. GATES, J. SEAGO, P. ANZ-MEADOR, Comparison of the NASA

ORDEM 3.1 and ESA MASTER-8 Models, Orbital Debris Quarterly News, 2021, Sept,v25i3.

[20]D. Wright, Space debris, Physics today,2007,10,35-40.

[21]TANG Zhi-mei, DING Zong-hua, DAI Lian-dong, WU Jian, XU Zheng-wen, "The Statistics Analysis of Space Debris in Beam Parking Model in 78° North Latitude Regions," Space Debris Research, 2017, 17,3, 1-7.

[22]TANG Zhimei DlNG, Zonghua, YANG Song, DAI Liandong, XU Zhengwen, WU Jian The statistics analysis 0f space debris in beam parking model based On the Arctic 500 MHz incoherent scattering radar, CHINESE JOURNAL 0F RADIO SCIENCE, 2018, 25,5, 537-542

[23]TANG Zhimei，DING, Zonghua，DAI Liandong，WU Jian，XU Zhengwen, Comparative analysis of space debris gaze detection based on the two incoherent scattering radars located at 69N and 78N, Chin．J．Space Sci, 2018 38,1, 73-78. DOI:10.11728/cjss2018.01.073

[24]DING Zong-hua, YANG Song, JIANG hai, DAI Lian-dong, TANG Zhi-mei, XU Zheng-wen, WU Jian， The Data Analysis of the Space Debris Observation by the Qujing Incoherent Scatter Radar, Space Debris Research, 2018, 18,1, 12-19.

[25]YANG Song, DING Zonghua, Xu Zhengwe, WU Jian, Statistical analysis on the space posture, distribution, and scattering characteristic of debris by incoherent scattering radar in Qujing, Chinese Journal of Radio science, 2018 33,6 648-654, DOI:10.13443/j.cjors.2017112301

[26]Clet Lab, Clet: a C compiler, https://drive.google.com/file/d/1OjKqANcgZ-9V5 6rgcoMtOu9w4rP49sgN/view?usp=sharing

[27]Huaiyang Cui, Relativistic Matter Wave and Its Explanation to Superconductivity: Based on the Equality Principle, Modern Physics, 10,3(2020)35-52. https://doi.org/10.12677/MP.2020.103005

[28]Huaiyang Cui, Relativistic Matter Wave and Quantum Computer, Amazon Kindle eBook, 2021.

[29]Huaiyang Cui, Evidence of Planck-Constant-Like Constant in Five Planetary Systems and Its Significances, viXra:2204.0133, 2022.

[30]Huaiyang Cui, Approach to enhance quantum gravity effects by ultimate acceleration, viXra:2205.0053, 2022.

[31]N.Cox, Allen's Astrophysical Quantities, Springer-Verlag, 2001, 4th ed..

[32] S. E. Schneider, T. T. Arny, Pathways to Astronomy, McGraw-Hill Education, 2018, 5th ed.

[33] https://en.wikipedia.org/wiki/El_Ni%C3%B1o%E2%80%93Southern_Oscillation

[34] https://en.wikipedia.org/wiki/Atmosphere_of_Earth

[35] WANG Hui, WANG Aimei , LI Wenshan , LUO Jinxin , ZHANG Jianli, ZUO Changsheng, Changes in key indicators of coastal marine climate in China, Marine Science Bulletin, 2021, 23(1):17-34.

[36] Liping Li et al, Introduction to Atmospheric Circulation, 2nd edition, Science Press, 2021,

[37] https://en.wikipedia.org/wiki/Tropical_cyclone

[38] https://en.wikipedia.org/wiki/Tropical_cyclone_basins

[39] (a) https://commons.wikimedia.org/wiki/File:Pacific_typhoon_tracks_1980-2005.jpg#/media/File:Pacific_typhoon_tracks_1980-2005.jpg).　(b) https://commons.wikimedia.org/wiki/File:Pacific_hurricane_tracks_1980-2005.jpg#/media/File:Pacific_hurricane_tracks_1980-2005.jpg.

[40] H.E.Willoughby, Gradient balance in tropical cyclones, Journal of the Atmospheric Science, 1990, Vol.47, 2, 263-274.

[41] Q.R.Xing,et al, Response of contemporary tree ring width of Cinnamomum camphora to climate change in Yangchun, Guangdong Province, Acta Ecologica Sinica, 2004, Vol.24,9,2077-2080.